

# Nanopores of a Covalent Organic Framework: A Customizable Vessel for Organocatalysis

Debanjan Chakraborty, Dinesh Mullangi, Chandana Chandran, and Ramanathan Vaidhyanathan\*

Cite This: *ACS Omega* 2022, 7, 15275–15295

Read Online

ACCESS |



Metrics &amp; More

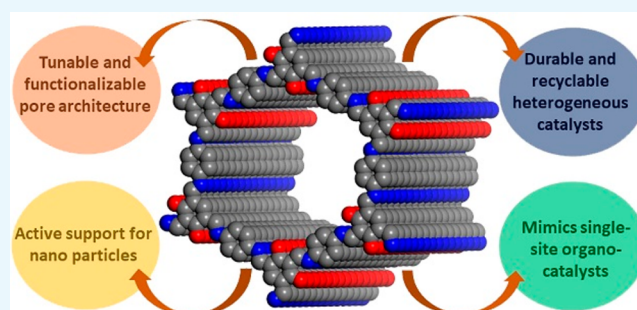


Article Recommendations



Supporting Information

**ABSTRACT:** Covalent organic frameworks (COFs) as crystalline polymers possess ordered nanochannels. When their channels are adorned with catalytically active functional groups, their highly insoluble and fluffy powder texture makes them apt heterogeneous catalysts that can be dispersed in a range of solvents and heated to high temperatures (80–180 °C). This would mean very high catalyst density, facile active-site access, and easy separation leading to high isolated yields. Different approaches have been devised to anchor or disperse the catalytic sites into the nanopores offered by the COF pores. Such engineered COFs have been investigated as catalysts for many organic transformation reactions. These range from Suzuki–Miyaura coupling, Heck coupling, Knoevenagel condensation, Michael addition, alkene epoxidation, CO<sub>2</sub> utilization, and more complex biomimetic catalysis. Such catalysts employ COF as a “passive” support that merely docks catalytically active inorganic clusters, or in other cases, the COF itself participates as an “active” support by altering the electronics of the inorganic catalytic sites through the redox activity of its framework. Even more, catalytic organic pockets or metal complexes have been directly tethered to COF walls to make them behave like single-site organocatalysts. Here, we have listed most COF-based organic transformations by categorizing them as metal-free non-noble-metal@COF and noble-metal@COF. The initial part of this review highlights the advantages of COFs as a component of a heterogeneous catalyst, while the latter part discusses all of the current literature on this topic.



## INTRODUCTION

Covalent organic frameworks (COFs), because of their ordered nanopores and crystalline structure, have become designable polymers. Their pores can be microporous or mesoporous by choosing the monomers of the desired length and geometry. Remarkably, the mesoporous COFs can be made to have a pore size as large as 65 Å,<sup>1</sup> something other metal-containing frameworks fail to accomplish due to the combined unfavorable effects of hydrolyzable metal–ligand bonds and a challengingly high void-to-framework ratio. Just like MOFs, COFs occur typically as fine polycrystalline powders but are a lot fluffier due to their lightweight all-organic backbone.<sup>2</sup> Such organic frameworks allow their amalgamation into various bulk materials such as polymers, papers, and textiles, imparting a micro-mesoporous structure to the composite.<sup>3a,b</sup> This new class of porous crystalline polymers possesses a modular design wherein the monomeric modules can be made to have specific geometry to decide the final framework to be a classic graphite-resembling layered  $\pi$ -stacked structure or zeolite-resembling 3D networks.<sup>1a–f</sup> The more abundant 2D COFs typically present a  $\pi$ -stacked layered structure held together by van der Waals or hydrogen bonds or C- $\pi$  type of interactions (Figure 1).<sup>3c–e</sup> Though their layer separations are comparable to graphite, the presence of larger pores within the layer make the interlayer stacking weaker.

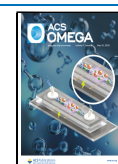
This becomes an advantage when it comes to exfoliation-assisted interlayer space accessibility.<sup>3f</sup> The stacked layers generate uniform periodic pores that are the true nanopores or containers wherein several chemistries can be staged.

While these are the structural advantages, the functional edge comes from the organic backbone. The modular framework facilitates the stoichiometric incorporation of chemically active sites. For example, it is well-known that the inclusion of heteroatoms such as N, P, and S into graphene markedly improves its catalytic ability by enhancing the ability to bind to substrates and, if necessary, to metallic nanoparticles.<sup>4</sup> However, typical C–N frameworks are synthesized via a high-temperature pyrolysis route that involves heating the graphene or carbonaceous source with small N-rich molecules at 350–800 °C under an inert atmosphere (Figure 2).<sup>4a</sup> This yields the desired C–N framework, but controlling the position of the N atoms or deciding the chemical nature of

Received: January 12, 2022

Accepted: April 5, 2022

Published: April 26, 2022



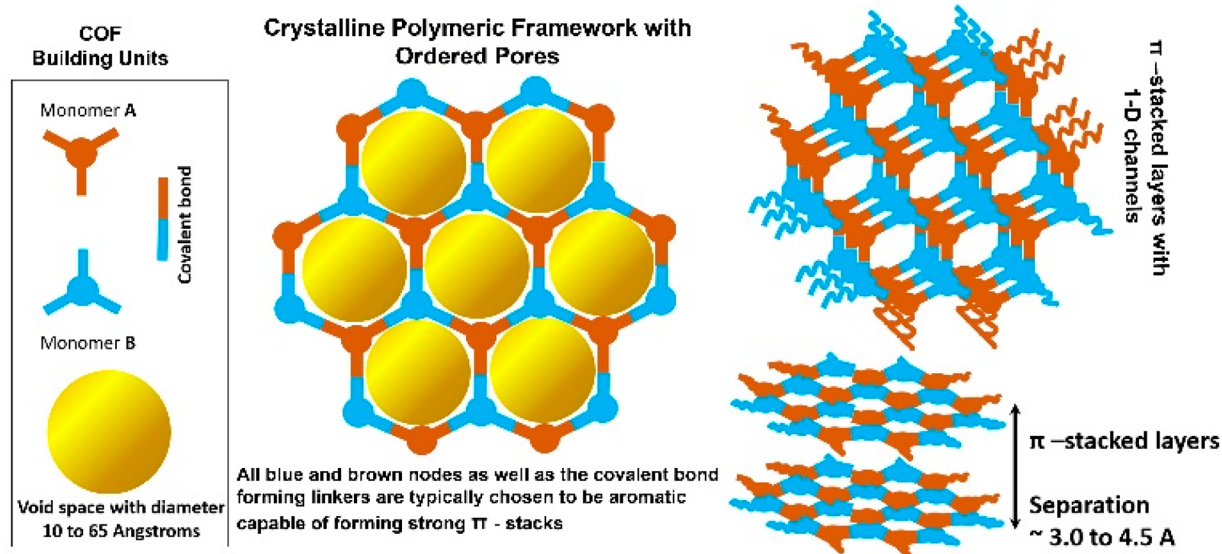


Figure 1. A schematic representation of an archetypal 2D-COF structure. The  $\pi$ -stacked layers with 1D channels are shown.

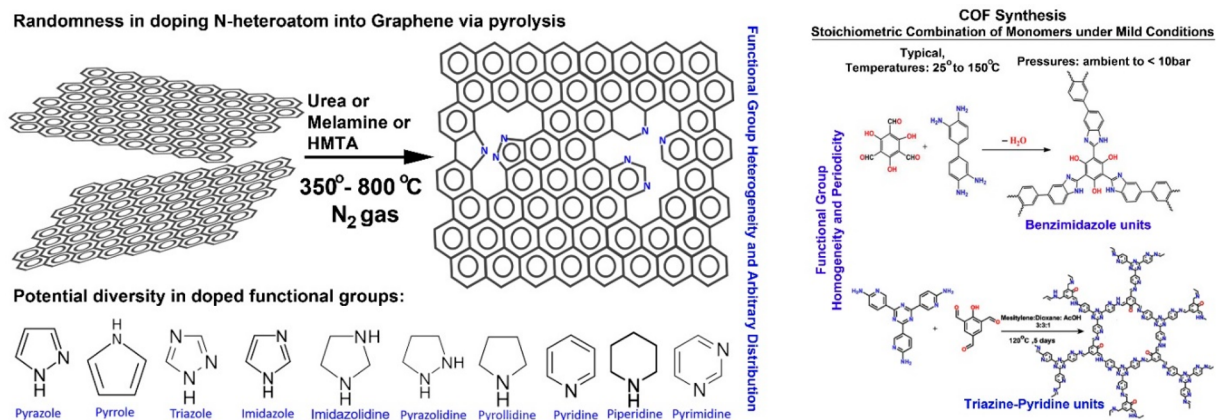


Figure 2. A schematic showing the superiority of COFs over carbon support in terms of catalytically important heteroatom doping.

the doped N atoms is not easy. In contrast, COFs are typically synthesized via soft chemical routes and form as crystalline powders. Hence, a high degree of functional group homogeneity and periodic arrangement is achieved. The highly insoluble nature of COF in a wide range of solvents, acids, and bases and their stability toward several chemical species even at high temperatures and pressures (80–130 °C, up to 10–20 bar) make them excellent candidates for heterogeneous catalyst development (Figure 2).<sup>1,2a–d,3c–f</sup>

Any metallic or metal-based catalyst's activity is typically enhanced when the catalyst is reduced to nanodimensions.<sup>5a–d</sup> However, homogeneous reactions where the nanoparticle or single-ion catalysts are used suffer from coagulation issues and difficulty in product isolation, which leads to lowered isolated yields. Also, rapid substrate binding-release and lack of substrate confinement leads to poor selectivity.<sup>5e,f</sup> Heterogeneous catalyst (solid-phase) can help overcome these issues. These have been pictorially represented in Figure 3.<sup>6a,b</sup> One can develop the heterogeneous catalyst involving these active nanoclusters via three different approaches: (i) by supporting the nanoclusters on a porous matrix.<sup>6c–e</sup> For this, metal-based nanoclusters or particles can be grown inside the porous support in a postsynthetic manner; (ii) by crystallizing the nanoclusters into a more robust but porous form (intrinsically

porous).<sup>6f,g</sup> This can be achieved by growing the catalytically active metal-based compounds in the presence of a sacrificial template, which can be removed postsynthetically; and (iii) by decorating the pores of the support with the active sites in a uniform periodic fashion.<sup>6h,i</sup> For example, a basic or acidic or chiral functional moiety can be tethered to the building unit or monomer that generates the polymeric framework, and such moieties typically protrude into the pore spaces, thus gaining maximum access. The challenges and advantages of each of these catalyst designs are presented in Figure 3. Of these different approaches, the third one is highly impactful in achieving maximum active-site participation and is easier to tune synthetically.

When we stabilize the inorganic catalytic entities on a crystalline porous support, there are two options. One is to make them single-site catalysts wherein the catalytically active metal-ion with labile groups is directly covalently coordinated to the COF framework (nonstoichiometric) or to render them as relatively larger nanoclusters that get anchored to the binding sites lining the pore walls, not necessarily via a strong covalent/coordinate bond (nonstoichiometric, in low weight percentages). This can expose the active facets of the nanocluster for substrate binding (Figure 4).<sup>7a,b</sup> Alternatively, if the catalytic moiety can be covalently tethered to the pore

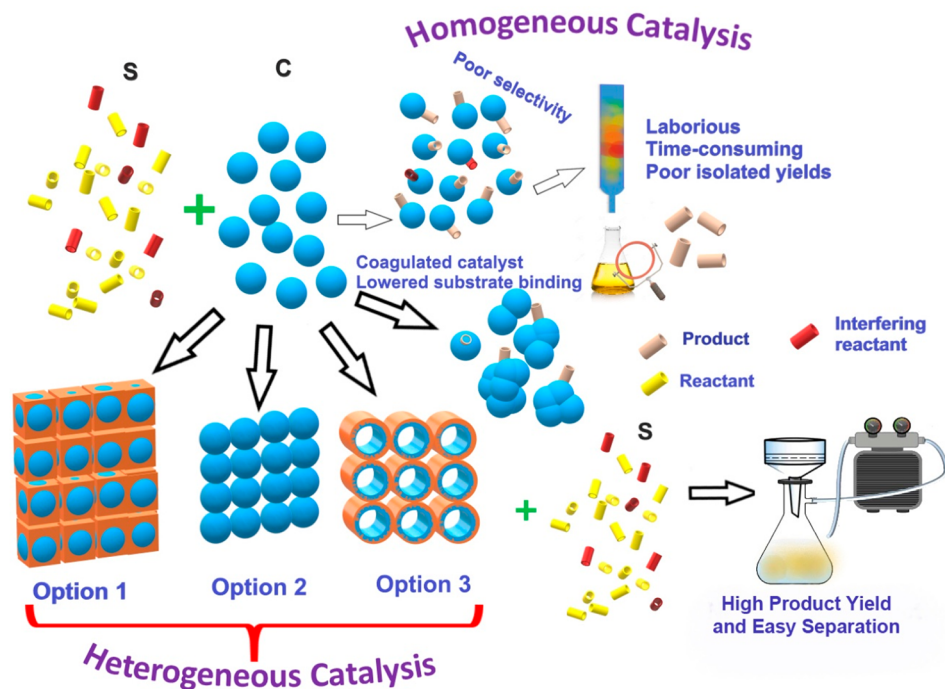
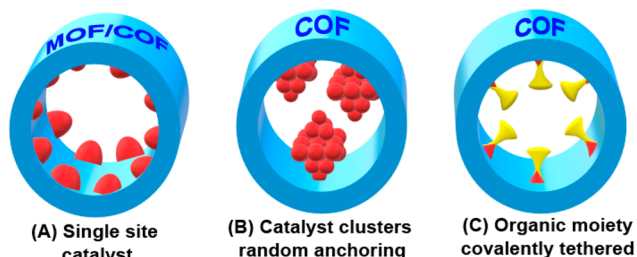


Figure 3. Homogeneous vs heterogeneous catalysts. Design of heterogeneous catalysts.



- \* Can be achieved in MOF and COF with ordered pores.
- \* Offers larger pores leaving sufficient porosity even after catalyst linking.
- \* Due to lack of hydrolyzable metal-ligand bonds, COF exhibit more chemical stability.

Figure 4. Different options to include catalytic sites into the COF.

walls of the support (stoichiometric or 100% loading),<sup>7c,d</sup> this would be most effective as it will ensure stability, and every site can participate in the catalysis (Figure 4).<sup>7d</sup> COFs meet most of these demands.<sup>1</sup> They can have large mesopores that will produce sufficient nanopores even after the catalytic appendages are anchored to them. Because of the lack of hydrolyzable bonds, they can be very stable to several reaction conditions.<sup>3c,d,7d</sup> Periodic pores will provide a uniform distribution of the catalytic sites.<sup>3c,d</sup>

Other advantages of COFs include the following.

**Chemical/Electronic Effects.** COFs could provide chemical and electronic interaction with the substrates of interest. This could be directed to a particular path of reaction. The electronic interaction can polarize a substrate which can enhance the reaction rate and subsequently yield. Weak VDW interactions (H-bonding,  $\pi$ - $\pi$  interaction, etc.) with the substrate also can lead to a particular thermodynamically controlled product.<sup>1,2a-d</sup>

**Effects on Metal Atoms.** Generally, heteroatoms present in the COF pore interact with the metal atoms/nanoparticles. These atoms can tune the Lewis acidity/basicity of a metallic species.<sup>3c,d</sup> For example, if sulfur/phosphorus is present in the

COF, then the metal can interact with the empty  $\sigma^*$  orbital of sulfur/phosphorus by back-bonding to tune the catalytic activity of the metal center. Also, if the framework of the COF has redox-active modules, they typically tend to express this as an electronic activity but only over a few repeat units. This is due to the intrinsic defects within the conjugated COF framework.<sup>3d</sup> However, even this relatively short-range conjugation-assisted redox activity would be able to communicate to the guest metal-based catalytic clusters or particles, boosting their activity.<sup>3d</sup> How loud they talk depends on the cluster's proximity to the framework sites and the ability of the heteroatoms to form a covalent or coordinate type interaction with the extra-framework metallic clusters.

**Tuning Biological Systems.** COFs can serve as a phase transfer catalyst for the reactions at biological systems. COF backbones decorated with amino acids/biological molecules (sugar, crown ethers, etc.) could provide a perfect nanoreactor for biological reactions. Porphyrin-based COFs could host the biologically active metal ions ( $\text{Fe}^{3+}$ ,  $\text{Mo}^{6+}$ ,  $\text{Zn}^{2+}$ , etc.) and mimic different enzymatic processes. The nanoporous architecture of COF has been used as the potential drug carrier for chemotherapy.<sup>8a-c</sup>

**Gas Capture and Conversion.** COFs with their inherent porosity are well-positioned for gas capture, storage, and conversion. They can host the catalytically active species (Lewis acidic metal/Lewis basic sites/nucleophiles) to interact with gaseous species. COF can provide nanoconfinement to support the activation of gaseous molecules like  $\text{CO}_2$ ,  $\text{NH}_3$ ,  $\text{CH}_4$ ,  $\text{N}_2$ ,  $\text{O}_2$ , etc., via increased intermolecular collisions. Activated gaseous species will undergo superior electron/energy transfer with the substrate to convert to valuable chemicals within these COF containers. This capture and conversion can be enhanced by tuning the pore architecture and introducing different organic and inorganic species in the COF.<sup>8d-f</sup>



Table 1. Selected Organic Transformation Catalyzed by Metal-free COFs

No.	COF Building units	Catalysed Reactions	Yield (%), TON, TOF (h <sup>-1</sup> )	Ref.
<b>Knoevenagel Reaction</b>				
1			96-98% when R=H	9b
2			92-98%	9c
3			>90%	9d
4			5-95% depending on the aldehyde and COF used.	9e
5			~70%	9f
<b>CO<sub>2</sub> Utilization</b>				
6			>90%	10c
7			>95%, TON >400 for cyclic carbonate formation and 40-90%, TON: 198-480 for cyclic amide formation.	10d
8			95-99%	10e
9			71-99%	10f



Table 1. continued

No.	COF Building units	Catalysed Reactions	Yield (%), TON, TOF (h <sup>-1</sup> )	Ref.
<b>Biomimetic Catalysis</b>				
10			>99%	11a
11		<p>The image for catalysed reaction has been reprinted with permission from the Wiley Online Library (Reference no. 11c).</p>	> 90% for HMF and 65% for DFF formation.	11c
<b>Michael addition and Diels-Alder Reaction</b>				
12			~50%	11f
13			63-98%	11g
14			60-90%	11h
<b>Phase-transfer Catalysis</b>				
15		<p>The image for catalysed reaction has been reprinted with permission from the Royal Society of Chemistry (Reference no. 11i).</p>	96% for the iodination reaction and 47-99% for nucleophilic substitution reaction.	11i

**Directing the Polymerization Reaction.** 2D COFs have a porous channel along a particular crystallographic axis. This could be advantageous to catalyze chain polymerization reactions. Moreover, the pore wall could block the branch polymerization of the monomer, thus enhancing the polydispersity and the weight-average/number-average molecular weights of the chain polymer. The heteroatoms in the COF pore walls, could catalyze the polymerization reaction.<sup>8g</sup>

Here, we have listed most of the COF-aided organic transformations categorized as metal-free, non-noble-metal@COF and noble-metal@COF.

## ■ METAL-FREE COFS AS CATALYSTS FOR ORGANIC TRANSFORMATIONS

It is indeed advantageous to carry out heterogeneous catalysis with a crystalline all-organic polymeric substrate; however, it is probably the most challenging. Introducing a basic site into the polymer is relatively straightforward; however, it is harder to incorporate Bronsted acid sites. This is because the crystalline organic frameworks typically form from reversible chemistry that assists the covalent bond formation and correction. However, such bonds are prone to hydrolysis catalyzed by strong acids and bases in an aqueous medium.<sup>1,2a-d</sup> Even some

degree of hydrolysis can significantly collapse the long-range order of the framework and nanochannels, instigating a rapid drop-in activity. Also, typically, inorganic catalysts such as nanosized metal clusters or oxides, nitrides, carbides, etc. generally exhibit high conductivity or electronic activity, realizing such activity levels in organic frameworks requires a high degree of defect-free conjugation.<sup>3d</sup> Given all these challenges, still very interesting organocatalysis has been affected using metal-free COF.

**Knoevenagel Condensation.** The condensation of carbon acid or esters with aldehydes has been used to afford  $\alpha,\beta$ -unsaturated compounds.<sup>9</sup> Wang and co-workers described a very interesting tetrahedral-tetramine and (3,3'-bipyridine)-6,6'-dicarbaldehyde (BPyDA)-based 3D COF with an interpenetrated structure (Table 1, entry 4).<sup>9e</sup> Still, it showed a dynamic behavior to gases and solvents. The framework expanded with the inclusion of solvent (THF ~35% increase of unit cell volume), with the dynamic framework having the pore size stretchable from  $5.8 \times 10.4 \text{ \AA}^2$  (contracted form) to  $9.6 \times 10.4 \text{ \AA}^2$  (expanded form) with solvent inclusion. The material shows such framework expansion to CO<sub>2</sub> gas as well. The dynamic nature has been attributed to the “pedal”-like rotation about the imine bonds. Knoevenagel condensation between aromatic aldehyde and malononitrile to yield benzylidene malononitrile was carried out to demonstrate the ability of the bipyridine groups to catalyze the reaction within the pore. Interestingly, their comparative study with the nonpyridine-containing isostructural COF showed that the pyridine COF gave a 72% yield in 6 h, outperforming COF-320 (42% yield)<sup>9e</sup> and nonporous analogue LZU-101 (21%, see Supporting Information for the synthesis)<sup>9e</sup> and achieved 99% yield in 10 h. However, there was no direct exploitation of the dynamic framework in these catalyzes. Similar size-dependent activity for ring-opening reactions as well as Knoevenagel condensations has been shown in nonpyridine 3D COFs (Table 1, entry 5),<sup>9f</sup> but, in comparison, their yields have only been moderate. Thus, the atomic-level inclusion of basic sites in COF can be an effective strategy to developing metal-free catalysts.

**CO<sub>2</sub> Conversion with Metal-free Catalyst.** Ionic liquids (ILs) such as imidazolium bromide are already known to interact well with CO<sub>2</sub> and have been used in several CO<sub>2</sub>-related processes (ionic-liquid CO<sub>2</sub> conversion).<sup>10a,b</sup> Exploiting this, Dong and co-workers came up with an interesting strategy of covalently anchoring ILs inside the hydrazine-linked COF (Table 1, entry 6).<sup>10c</sup> IL-COF showed good CO<sub>2</sub> adsorption characteristics, and to add practical utility, they composited this IL-COF with readily available bulk material, namely, chitosan, a sugar-based polymer found in crustaceans.<sup>10c</sup> The aerogel of the composite could be molded to different shapes (with up to 80 wt % COF loading). In a creative attempt, a cup made out of this composite was utilized as a fixed bed reactor to catalyze the conversion CO<sub>2</sub> to cyclic carbonates in a solvent-free manner with good yields at 80 °C, over 48–72 h. In a separate study,<sup>10d</sup> they converted CO<sub>2</sub> into oxazolidinones using porphyrin-based COFs as catalysts (Table 1, entry 7). Several oxazolidinones formed in good yield with excellent regio-selectivity and TON (Avr.  $\approx$  450).

Han and co-workers loaded “betaine” species (trimethylglycine) as the zwitterionic guest into the pores of a hydroxyl functionalized COF.<sup>10e</sup> They reacted the discrete betaine units counterbalanced by electrophilic alkyl bromine groups with the hydroxyl units lining the COF via Williamson ether formation (Table 1, entry 8). This covalently links the betaine units to

the COF. Now, utilizing PhSiH<sub>3</sub> capable of forming hyper-valent silicon species via interaction with the oxygen atom of betaine and by varying the conditions (the pressure of CO<sub>2</sub>, ambient to 5 to 10 bar), they hierarchically reduced the CO<sub>2</sub> to formamide, methylamine, and aminal. The amine units of the betaine moieties in the COF serve as the activation sites for the CO<sub>2</sub>. High conversion and selectivity were observed for each of the products. Liu and co-workers reported highly crystalline, mesoporous, and stable COFs with many hydroxyl groups decorating their pore walls. The COFs catalyze the cycloaddition of CO<sub>2</sub> to substituted epoxides forming cyclic carbonates under mild conditions. The hydroxyl groups on the pore wall provide the binding sites for the substrate and the CO<sub>2</sub> leading to the products with significant enhancement of the yields (Table 1, entry 9).<sup>10f</sup> Thus, COFs have proven to be an effective catalyst for CO<sub>2</sub> capture and conversion.

**Biomimetic Catalysis.** Ma and co-workers described a creative approach toward forming a dynamic catalyst by arraying the pores of a sulfonated-COF with flexible linear-chain polymer, namely, the polyvinylpyrrolidone (PVP) (Table 1, entry 10).<sup>11a</sup> The spatial environment of such COF pores mimics the outer-sphere residue cooperativity within the active sites of enzymes. This catalyst design benefits from the flexibility and enriched concentration of the functional moieties on the linear polymers. Specifically, in the representative dehydration of fructose to produce 5-hydroxymethylfurfural, dramatic activity and selectivity improvements have been achieved [catalyst, PVP@[SO<sub>3</sub>H]<sub>0.17</sub>-COF (comparative values obtained for *p*-toluenesulfonic acid as a catalyst are shown in brackets): Time = 30 min; conversion = >99.5 (28.5); selectivity = 99.1 (73.5); yield = 99.1 (20.9)]. The superiority of the COF catalyst originates from well-thought-out design aspects. De facto, the system incorporates a few smart design choices. For example, the COF utilized is methoxy-stabilized, with enormous chemical stability due to interlayer hydrogen bonds and C- $\pi$  and  $\pi$ - $\pi$  stacking interactions, all of which enable the functionalization of this imine-COF with highly acidic sulfonic acid groups, a strategy employed in another catalytic imine-COF.<sup>11b</sup> The COF retains complete crystallinity even upon sulfonation. The acidic walls of the COF are made to cooperatively function with the pyrrolidone, which is well-established from a series of control studies. The COF was chosen with large mesopores to ensure sufficient openness even in the polymer-loaded form, which gives unhindered access to the active sites of the linear chain polymer.<sup>11a</sup>

**Fructose to Furfural and Formyl-furan.** Zhao and co-workers described a sulfonated 2D imine-COF, termed TFP-DABA, synthesized directly from 1,3,5-triformylphloroglucinol and 2,5-diaminobenzenesulfonic acid (Table 1, entry 11).<sup>11c</sup> The irreversible enol-to-keto tautomerization guaranteed structural stability. TFP-DABA is a highly efficient solid acid catalyst for fructose conversion with remarkable yields (97% for 5-hydroxymethylfurfural and 65% for 2,5-diformylfuran or formylfurfural), good chemoselectivity, and good recyclability. Notably, the PXRD and the porosity studies indicate that the COF is not necessarily well formed, and this can be expected as an imine-bond has to coexist with highly acidic sulfonic acid moieties, leading to the possibility of a defective structure with lowered long-range order.<sup>11c</sup> The control experiments performed in the absence of the COF support showed that though the kinetics were better for the homogeneous

Table 2. Non-Noble-Metal-Based COF Catalysts

No.	COF Building units	Catalysed Reactions	Involved Metal and Oxidation State	Yield (%), TON, TOF (h <sup>-1</sup> )	Ref.
<b>Oxidation Reaction</b>					
1			Mo(VI)	~17-99%. TOF: 16-162 h <sup>-1</sup> .	12b
2			Mo(VI)	71-99%	12c
3			Cu(II)	5-90%, TOF: 5-20 h <sup>-1</sup> .	12d
4			Co(II) and Mn(II)	60-99%	12e
5			Fe(III) and Mo(VI)	50-88%	12f
6			Mn(II)	20-99%	12g
<b>Glaser-Hay Coupling</b>					
7			Cu(0) and Cu(I)	~70%, TON: 160-190, TOF: ~50 h <sup>-1</sup>	13a
<b>Chan-Lamcoupling</b>					
8			Cu(II)	>80%	13c



Table 2. continued

No.	COF Building units	Catalysed Reactions	Involved Metal and Oxidation State	Yield (%), TON, TOF (h <sup>-1</sup> )	Ref.
<b>Prins Reaction and Mannich-Type Reaction</b>					
9		Prins condensation: 	V(V)	>90%	13e
10		Mannich-Type Reaction 	V(V)	>90%	13f
<b>Cross Coupling Reaction</b>					
11		Decarboxylative cross-coupling reaction: 	Fe(III)	28-80%	14b
12		Suzuki-Miyaura cross-coupling: 	Ni(II)	~34%	14c
<b>Reductive Cleavage of C-S Bond or Desulfurization, Nitro/Nitrile Reduction Reaction</b>					
13			Ni(0)	9-99%	14e
14			Co(0) and Co(II)	68-87%, TON: 47-60	11b
<b>Cyanosilylation of Aldehydes</b>					
15			Mn(II)	>95%	14f

conditions, and the conversion and selectivity were far superior when the COF was employed as the catalyst.

**Michael Addition.** The Michael addition is the nucleophilic addition of a carbanion or another nucleophile to an  $\alpha,\beta$ -unsaturated carbonyl compound functionalized with an

electron withdrawing group. It belongs to the larger class of conjugate additions.<sup>11d,e</sup> This is one of the most useful methods for the mild formation of C–C bonds. Of the different options available for introducing catalytic sites, as can be seen, the incorporation of inorganic nanoparticles is rapid

and versatile. However, it does not guarantee homogeneity of sites and geometry at the metal site or the uninterrupted access. Developing a single-site catalyst could be a nice alternative, but since they are typically organometallic complexes, they can leach during multiple cycles of catalysis. Given these, the best option is to have reaction specific organocatalytic sites covalently tethered to the skeleton of the framework. In fact, this can even be stoichiometric. The only concern would be the cost involved in the multistep synthesis of such metal-free organocatalysts.

The effectiveness of this approach is excellently articulated by the work of Jiang and co-workers.<sup>11f</sup> They have appended pyrrolidine derivatives capable of catalyzing Michael addition reactions to the COF walls using two-step click reactions. They showed that the inclusion of the ethynyl groups (attached to the backbone of the 4,4'-aldehyde forming the linear linker) could be done with a great degree of control and was monitored by a systematic decrease in the surface area and pore size. Thus, it formed a pyrrolidone-functionalized COF catalyzed Michael addition reaction (Table 1, entry 12). A comparison is made to the homogeneous reaction done using (*S*)-4-(phenoxyethyl)-1-(pyrrolidin-2-ylmethyl)-1*H*-1,2,3-triazole as a control. Impressively, the 3.3 h to 100% conversion in the homogeneous medium was reduced to 1 h for the COF-based catalyst. The stereoselectivity improved with bulkier pyrrolidone substituents. Most importantly, when analogous nonporous or amorphous polymers were used, the reactivity was sluggish and took 65 h to complete. Going one step further, they demonstrate that the COF could be loaded into a column of a continuous flow reactor and 100% conversion with good ee and dr values could be obtained. With such methods, even if the initial cost of the synthesis of the COF-derived catalyst is high, one may be able to tackle it by reusability over several cycles. Zhang and co-workers reported a squaramide COF with pore walls uniformly lined by the C=O groups of the squaramide moieties (Table 1, entry 13).<sup>11g</sup> These hydrogen bonding centers catalytically controlled the Michael addition reaction between the  $\beta$ -nitrostyrene and 2,4-pentanedione. A control COF with comparable structure but devoid of squaramide units did not work.

COFs are also utilized for catalyzing the Diels–Alder reaction. Jiang and co-workers reported a COF having pore walls made up of  $\pi$  electron-rich aromatic rings that promote the Diels–Alder reaction with excellent yield and recyclability (Table 1, entry 14).<sup>11h</sup> Similarly, COFs decorated with crown ethers can serve as potential candidates for phase transfer catalysts. Zhao and co-workers have reported such an 18C6 functionalized COF to catalyze the iodination of 1-bromooctane under a solid–liquid–solid condition (Table 1, entry 15).<sup>11i</sup>

## ■ NON-NOBLE METAL DECKED COF FOR ORGANOCATALYSIS

**Epoxidation/Selective Epoxidation of Olefin as a Model Reaction for M@COF (M = Mn, Co, Mo).** Finding non-noble metal-based heterogeneous catalysts is probably the keenest approach considering its cost-effectiveness, relative abundance, ease of synthesis and scalability, achieving high-activity, and optimal space-time yields.<sup>12a</sup> Oxidation/epoxidation of olefin is one of the well-studied model reactions for demonstrating the use of non-noble-metal-containing COFs.<sup>12b–g</sup> Inspired by biological systems, molybdenum catalysts mirroring peroxidase have been prepared by

anchoring Mo centers into a hydrazine-linked COF with a high active-site density (2.0 mmol g<sup>-1</sup>) (Table 2, entry 2).<sup>12c</sup> The Mo content of Mo-COF was 5–10 times higher than for systems such as Mo-complex grafted mesoporous sieve, MWCNT, and polymer.<sup>12c</sup> The anchoring to a support prevents the problem of metal-dimerization known to happen in a homogeneous medium, while catalyzing the olefin epoxidation, where the Mo-COF adopts different oxidation states resembling MoO<sub>2</sub>(*acac*)<sub>2</sub> complexes and also offers flexible coordination geometries. The epoxidation of different olefin substrates of various molecular sizes was also investigated. Their observations indicate that the COF catalyst exhibits reagent size selectivity (cyclohexene vs cyclooctene) confirming that the oxidation reaction indeed occurs inside the nanochannel of the framework. In another work, the Cu<sup>2+</sup> anchored to the imine and hydroxyl groups of a COF was employed as a catalyst for selective oxidation of olefins to aldehyde (Table 2, entry 3).<sup>12d</sup> A comparison was made between the neat COF versus Cu<sup>2+</sup>-loaded COF. The latter improved the conversion (20 vs 44), but the selectivity for benzaldehyde over styrene oxide does go down (81:0 vs 72:16). The Cu@COF offered some pore-size restrictions to the larger olefins, and this could be important when it comes to gaining more conversion of the olefin.

Impelled by the porphyrin-ring functionalized cytochrome P450 enzymes, which can efficiently activate dioxygen under mild conditions, a porphyrin-based COF was made as a mimic. They pinned the metals Mn or Co into the COF and employed a green aerobic oxidation to convert olefins into epoxides under ambient conditions using isobutyraldehyde (IBA) (Table 2, entry 4).<sup>12e</sup> Excellent conversion was obtained, and the TON for the styrene conversion to 1,2-epoxyethylbenzene could be increased to as high as 30 000 without any loss in activity (TOF: 3434 h<sup>-1</sup>). They proposed a curious mechanism wherein, at first, cobalt-porphyrin reacts with IBA to generate an acyl radical [(CH<sub>3</sub>)<sub>2</sub>CHC(O)•], which would react with O<sub>2</sub> to produce an acylperoxy radical [(CH<sub>3</sub>)<sub>2</sub>CHC(O)OO•] to realize molecular oxygen activation. Subsequently, the acylperoxy radical reacts with an olefin molecule to form an epoxide. For all substrates, the Co catalyst was superior over Mn. Though a mechanism has been proposed, having EPR or ESR based evidence for the free-radical would have been resounding.

In many of these M@COF-based catalysis, the role or the requirement of a COF as a structured porous support has been validated by utilizing control experiments without the catalyst, and also in some cases a simple technique such as UV–vis before and after the insertion of the substrate and extraction of the products has been used to support the mechanisms within reason.<sup>12e–h</sup> The highly insoluble nature of these polymeric COFs make mechanistic studies extremely challenging. In many cases, the pre- and postcatalysis XPS have been used to identify the metal oxidation states and have been compared to the robustly established metal oxidations states from solution-based homogeneous catalysis. However, further in situ methods and smarter time-frozen-analysis methods need to be incorporated to gain true insights into the mechanism of action (Table 2, entry 7).<sup>13a</sup> It is important to consider that the nanoconfinement obligated by the COF pores itself could lead to different types of mechanisms involving unlike intermediates compared to the homogeneous catalysis performed using the same metal catalysts.

**Chan–Lam Coupling.** Chan–Lam coupling is typically a copper complex-catalyzed cross-coupling reaction between an aryl boronic acid and an alcohol or an amine to form the corresponding secondary aryl amines or aryl ethers.<sup>13b</sup> Since it can be carried out in air at room temperature, it is more attractive over the popular Buchwald–Hartwig coupling which relies on the use of palladium. Zhang and co-workers<sup>13c</sup> have carried out a thorough investigation of a reaction between aryl boronic acids and amines (Table 2, entry 8). They developed a Cu@COF catalyst using a stable and cheap polyimide COF. They observed clear solvent dependency in the reactions; for example, the reaction does not proceed in ethyl acetate or ethyl lactate but occurred in THF, water, toluene, CH<sub>3</sub>CN, and dichloromethane with yields increasing in the same order. They could amplify the phenylboronic acid coupling with aniline from 1 to 20 mmol without any loss of yield (92%). The work has been expansive in covering a whole range of aliphatic, aromatic, and allylic substrates on the amine and some on the boronic acid.<sup>13d</sup> Every reaction has been backtracked to the benchmark high-performing non-COF catalyzed reaction. However, the powder pattern suggests that the polyimide may not be a highly polymerized cross-linked COF.

**Prins Reaction.** The Prins reaction is the acid-catalyzed addition of aldehydes to alkenes or alkynes, and the product can be a diol, dioxin, or allylic alcohol depending on the reaction conditions.<sup>13e</sup> Both protic acids such as H<sub>2</sub>SO<sub>4</sub> and Lewis acids such as AlCl<sub>3</sub> and even phosphomolybdic acids can be used as a catalyst. Ma and co-workers demonstrated the use of a vanadium-docked 1,2-diol functionalized COF for the reaction between an alkene and aldehyde (Table 2, entry 9).<sup>13e</sup> They synthesized nopol, an important bicyclic primary alcohol used in pesticides, detergents, perfumes, etc.<sup>13e</sup> The V@COF catalyzes also the oxidation of sulfides. Interestingly, the surface area and pore-volumes of the COF do not change after the loading of vanadium. It appears that if there are extremely well-defined sites in the COF which can bind to a specific metal complex wherein the metal has a well-defined oxidation state, the metal simply becomes part of the framework and hence does not fill up the pores. In these cases, they are single-site catalysts. However, the catalytic efficiency is not 100%, which indicates that even in such cases, all the sites in the COF framework may not be binding to the metal or the access to the metal-ion is probably restricted owing to the layer slippage or other defects in the COF. The same researchers used the same vanadium-docked COF to catalyze a Mannich-type reaction between beta-naphthol and 4-methylmorpholine N-oxide (NMO) to make Mannich bases in high yields (Table 2, entry 10).<sup>13f</sup> In both cases, they proposed a plausible mechanism at the docked vanadium sites.

**Cross-Coupling Reactions Using Non-Noble-Metal-Decorated COFs.** *Decarboxylative Cross-Coupling between Cinnamic Acid and 1,4-Dioxane.* Developing non-noble-metal-based heterogeneous catalysts to replace Pd-based catalysts in cross-coupling C–C bond forming reactions is always topical. This is because such cross-coupling organic reactions dominate all areas of materials science. Decarboxylative cross-coupling reactions involve a reaction between carboxylic acid and an organic halide to form a new carbon–carbon bond by removing HX, concomitant with loss of CO<sub>2</sub>. Typically, a metal catalyst, base, and oxidant are required.<sup>14a</sup> Of all, the iron-based catalyst is one of the most sorted out targets owing to its undeniable diverse advantages. However,

even the heterogeneous iron catalyst, under a solvent medium, during the catalysis, behaves like a wild horse. This is due to a variety of oxidation states that the iron adopts and also due to their irreversible or nonlabile coordinations and due to the high solubility of certain in situ generated redox species (causes catalyst leaching). Most importantly, there is a library of complexes/compounds of iron forms responding to the mild changes in localized environments of the reaction medium, which makes it hard to ascertain active species directing the action. This makes the mechanistic understanding very difficult, which impacts the design, scalability, and reproducibility. Recently, a COF-supported FeCl<sub>3</sub> has been employed as a catalyst in the decarboxylative cross-coupling between cinnamic acid and 1,4-dioxane using *tert*-butyl-hydroperoxide (TBHP) or *di**tert*-butyl-peroxide (DTBP) as an oxidant (Table 2, entry 11).<sup>14b</sup> The COF lost significant crystallinity upon loading FeCl<sub>3</sub> but retained the structural integrity. The Fe<sup>3+</sup> centers are proposed to bind to both in-layer and across-layer atoms. The BET surface area decreased from 1200 to 235 m<sup>2</sup>/g upon FeCl<sub>3</sub> loading (7.85 wt %). The activity drops with multiple cycles. Interestingly, when different substituted cinnamic acids were tried, it was observed that the reaction progressed only when the FeCl<sub>3</sub>@COF was used, and neat FeCl<sub>3</sub> salt did not yield any product.<sup>14b</sup> Also, the use of any inorganic oxidizing agents such as H<sub>2</sub>O<sub>2</sub> and K<sub>2</sub>Cr<sub>2</sub>O<sub>7</sub> in place of TBHP in the FeCl<sub>3</sub>@COF reaction medium drastically hampered the reaction. An organic peroxide formation was followed by heat-assisted generation of the reactive alkyl oxide free radical, which attacks the 1,4-dioxane molecule to form the 1,4-dioxane radical, which reacts with the cinnamate species bound to the Fe<sup>3+</sup> site embedded in the framework.<sup>14b</sup> This yields the C–C bond formation between the 1,4-dioxane and the cinnamate carbon followed by decarboxylation to yield the desired product. The lability of the Cl at the Fe(III) site is crucial. Though it has been found that the neat FeCl<sub>3</sub> is not able to catalyze this, it is not clear as to why it works when anchored to the COF.<sup>14b</sup>

*Suzuki–Miyaura Coupling.* Suzuki–Miyaura coupling is typically a Pd-catalyzed reaction between an alkenyl (vinyl), aryl, or alkenyl organoborane (boronic acid or boronic ester, or special cases with aryl trifluoroborane) and halide or triflate under basic conditions. This creates carbon–carbon bonds to produce conjugated systems of alkenes, styrenes, or biaryl compounds. A NiCl<sub>2</sub> was anchored into a specifically designed imine-phenol lined COF (Table 2, entry 12).<sup>14c</sup> This pocket is known to bind extremely well with Ni<sup>2+</sup> to form complexes.<sup>14d</sup> These units amalgamated into the COF backbone were shown to bind extremely well to the NiCl<sub>2</sub>, and no leaching was observed. Unfortunately, their performance toward C–C bond coupling Suzuki–Miyaura reactions showed only a moderate yield, and this could be due to the inherent slowness of Ni<sup>2+</sup> toward catalyzing such nonradical pathway-based C–C bond formation, especially in the heterogeneous phase. Also, its binding could be too strong impeding the required lability.

*C–S Bond Cleavage Hydrodesulfurization.* The reductive cleavage of C–S bonds helps sulfur cleanup from petroleum feedstocks. Classically, Pd, Rh/Ir, Ni(COD) complexes have been used as homogeneous catalysts for this reaction; when the inexpensive Raney nickel is employed, it significantly drops activity after the first reduction. McGrier and co-workers, exploiting the ability of dehydrobenzoannulene (DBA) units to bind to low-oxidation state first-row transition metals, deliberately used it in the COF construction using Ni(COD)



Table 3. Noble-metal@COF as a Heterogeneous Catalyst for Organic Transformations

No.	COF Building units	Catalysed Reactions	Involved Metal and Oxidation State	Yield (%), TON, TOF (h <sup>-1</sup> )	Ref.
<b>Bifunctional Catalysts using pre-designed pyridine groups in COF framework</b>					
1			Pd(0)	91-99%	15a
2			Rh(I) and Pd(II)	85-99%	15b
3			Pd(II)	~ 70%, TON: 1101	15c
<b>Reduction reaction using noble metal nanoparticles @COF</b>					
4			Pd(0) and Pt(0)	>95% for nitrophenol reduction and >99% for the coupling reaction>	16a
5			Au(0)	TOF: 2.7 h <sup>-1</sup>	16b
6			Au(0)	>99%	16c
7			Pd(0)	Removal rate of o-DCB is 90%.	16d
8			Au(0)	-	16e
9			Rh(0)	TOF: 505 min <sup>-1</sup>	16f

Table 3. continued

No.	COF Building units	Catalysed Reactions	Involved Metal and Oxidation State	Yield (%), TON, TOF (h <sup>-1</sup> )	Ref.
<b>Reduction reaction using noble metal nanoparticles @COF</b>					
10		<p>(a) </p> <p>(b) </p> <p></p> <p>The image for catalysed reactions has been reprinted with permission from the Wiley Online Library (Reference no. 16g).</p>	Pd(0), Pt(0) and Au(0)	>99% for all the reactions. TOF is 155-1648 h <sup>-1</sup> for the Suzuki-Miyaura coupling reaction.	16g
11		<p></p> <p>Selective formic acid dehydrogenation.</p>	Ru(IV), Ru(0)	>90%	16h
12			Au(0)	>99%	16i
13			Ag(0)	>90%	16j
14			Au(0)	>90%	16k
<b>Suzuki-Miyaura Coupling</b>					
15			Pd(II), Pd(0)	Yield: ~50-100%, TON: 400-1000 and TOF: 50-3000 h <sup>-1</sup>	17a
16			Pd(0)	~55-100%	17b

Table 3. continued

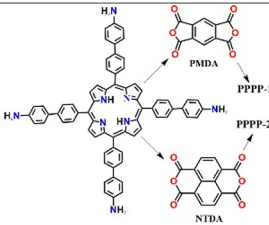
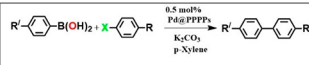
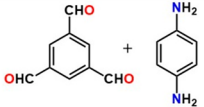
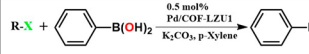
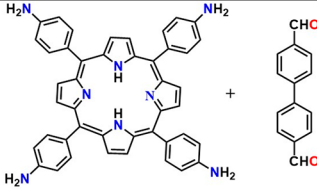
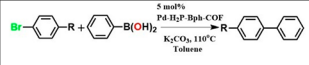
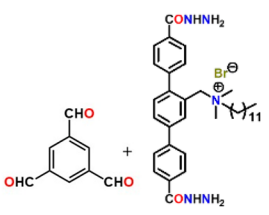
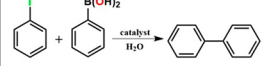
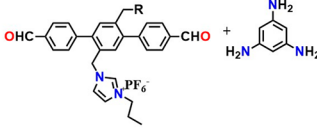

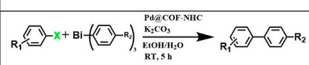
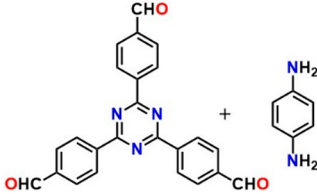
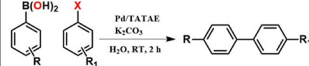
No.	COF Building units	Catalysed Reactions	Involved Metal and Oxidation State	Yield (%), TON, TOF (h <sup>-1</sup> )	Ref.
<b>Suzuki- Miyaura Coupling</b>					
17			Pd(0)	>90%	17c
18			Pd(II)	> 95%	17d
19			Pd(II)	>90%	17e
20			Pd(0)	~ 90%	17f
21			Pd(II)	>95% for Suzuki-Miyaura Cross Coupling and >80% for Crosscoupling reaction of triarylbi-muths and aryl halides	17g
					
22			Pd(II)	Yield: >90% TON: >1000	17h



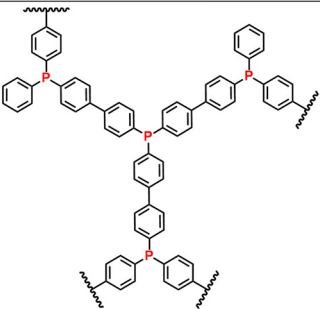
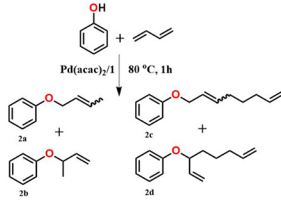
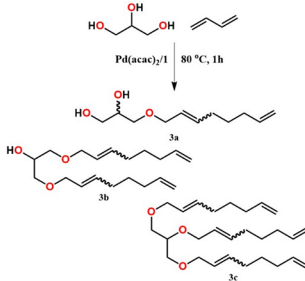
Table 3. continued

No.	COF Building units	Catalysed Reactions	Involved Metal and Oxidation State	Yield (%), TON, TOF (h <sup>-1</sup> )	Ref.
<b>Sonogashira coupling, and Heck coupling reactions</b>					
23		<p>(a) Sonogashira coupling between aryl iodides and aromatic/aliphatic alkynes.</p> $R-\text{C}_6\text{H}_4-\text{I} + \text{R}'-\text{C}\equiv\text{C}-\text{H} \xrightarrow{\text{Pd(0)}\text{@[TpPa-1]}} \text{R}'-\text{C}\equiv\text{C}-\text{C}_6\text{H}_4-\text{R}$ <p>(b) Heck coupling reaction between aryl iodides and aromatic/aliphatic olefins.</p> $R-\text{C}_6\text{H}_4-\text{I} + \text{R}'-\text{C}=\text{C}-\text{H} \xrightarrow{\text{Pd(0)}\text{@[TpPa-1]}} \text{R}'-\text{C}=\text{C}-\text{C}_6\text{H}_4-\text{R}$ <p>(c) One-pot sequential Heck/Sonogashira coupling reactions of aryl dihalides.</p> $\text{I}-\text{C}_6\text{H}_4-\text{Br} \xrightarrow{\text{Pd(0)}\text{@[TpPa-1]} \text{ (a)}} \text{R}-\text{C}_6\text{H}_4-\text{Br} \xrightarrow{\text{Pd(0)}\text{@[TpPa-1]} \text{ (b)}} \text{R}-\text{C}_6\text{H}_4-\text{C}\equiv\text{C}-\text{C}_6\text{H}_4-\text{R}$	Pd(II), Pd(0)	<p>(a) Yield: ~50%; TON: ~300, TOF: ~50 h<sup>-1</sup></p> <p>(b) Yield: ~90%; TON: ~300, TOF: ~50 h<sup>-1</sup></p> <p>(c) Yield: 62% and 85%; TON: 66 and 73, TOF: 11 and 12 h<sup>-1</sup></p>	18a
24		<p><b>Pd catalytic step</b></p> $\text{I}-\text{C}_6\text{H}_4-\text{I} + \text{R}'-\text{C}\equiv\text{C}-\text{H} \xrightarrow[\text{K}_2\text{CO}_3, \text{ACN}, 350\text{K}, \text{N}_2]{\text{MaPdgCOF}} \text{R}'-\text{C}\equiv\text{C}-\text{C}_6\text{H}_4-\text{I}$ <p><b>Mn catalytic step</b></p> $\text{R}'-\text{C}\equiv\text{C}-\text{C}_6\text{H}_4-\text{I} \xrightarrow[\text{MaPdgCOF}]{\text{IBA}, 290\text{K}, \text{air}} \text{R}'-\text{C}\equiv\text{C}-\text{C}_6\text{H}_4-\text{C}\equiv\text{C}-\text{H}$	Mn(II), Pd(II)	>90%	18b
25		$\text{R}'-\text{C}=\text{C}-\text{H} + \text{COF} \xrightarrow[\text{DMA, O}_2, 40^\circ\text{C}, 48 \text{ hr}]{\text{COF BTDI (5 mol\%)} \text{ Pd(OAc)}_2 \text{ (5 mol\%)} \text{ Cu(OAc)}_2 \text{ (20 mol\%)}} \text{R}'-\text{C}=\text{C}-\text{COF}$	Cu(II), Pd(II)	83-100%	18c
26		$\text{Br}-\text{C}_6\text{H}_4-\text{I} + \text{R}'-\text{C}=\text{C}-\text{H} \xrightarrow[\text{NMP, 120}^\circ\text{C, 1-10h, air}]{\text{Sodium acetate, catalyst}} \text{R}'-\text{C}=\text{C}-\text{C}_6\text{H}_4-\text{I}$	Pd(0)	82-97%, TON: 452-2473, TOF: 452-2473 h <sup>-1</sup>	18d
<b>CO<sub>2</sub> utilization</b>					
27		$\text{R}_1-\text{C}\equiv\text{C}-\text{C}(\text{OH})(\text{R}_2)-\text{H} \xrightarrow[\text{CO}_2, 1 \text{ atm}]{\text{Ag@[3D-HNU5]}} \text{R}_1-\text{C}\equiv\text{C}-\text{C}(\text{O})_2-\text{C}(\text{R}_1)(\text{R}_2)-\text{H}$	Ag(0)	Yield >99%, TON: 990	19a
28		$\text{R}_3-\text{C}\equiv\text{C}-\text{C}(\text{OH})(\text{R}_1)(\text{R}_2)-\text{H} \xrightarrow[\text{CO}_2, 4 \text{ hours}]{\text{Ag@[COF] DMF, DBU}} \text{R}_3-\text{C}\equiv\text{C}-\text{C}(\text{O})_2-\text{C}(\text{R}_1)(\text{R}_2)-\text{H}$	Ag(0)	85-97%, TOF: 152-172, TOF: 38-43 h <sup>-1</sup>	19b

Table 3. continued

No.	COF Building units	Catalysed Reactions	Involved Metal and Oxidation State	Yield (%), TON, TOF (h <sup>-1</sup> )	Ref.
Other important reactions (silicon based cross coupling, benzyl alcohol oxidation, bio catalysis, rearrangement etc.)					
29			Pd(II)	Yield: 70 to 90%	20a
30			Ru(0)	>90%	20b
31		$(GL)\text{-Cu(II)} \xrightarrow{\text{AgCOF}} \text{Cu}_2\text{O}$ GL: Glucose	Ag(0)	-	20c
32		 1a: R=H, n=1 1b: R=H, n=0 1c: R=CH3, n=1 2a: R=H, 92% 2b: R=OMe, 72% 2c: R=CF3, 77% 2d: R=Me, 80% 2e: R=Cl, 86% 2f: R=OH, 58% 2g: R=OMe, 92% 2h: R=CF3, 83% 2i: R=Me, 56% 2j: R=Cl, 68% 2k: R=NO2, 54%2l: R=OH, 58%	Pd(II)	54-92%	20d
33			Ir(I)	50-87%	20e

Table 3. continued

No.	COF Building units	Catalysed Reactions	Involved Metal and Oxidation State	Yield (%), TON, TOF (h <sup>-1</sup> )	Ref.
Other important reactions (silicon based cross coupling, benzyl alcohol oxidation, bio catalysis, rearrangement etc.)					
34		<p>Telomerisation of 1,3-butadiene with Phenol.</p>  <p>Telomerisation of 1,3-butadiene with glycerol&gt;</p> 	Pd(II)	Conversion 84%	55-20f

as the source (Table 2, entry 13).<sup>14e</sup> About 8.56% of Ni was loaded, which corresponded to utilizing 64% of the DBA units. Surprisingly, there was not much drop-in the surface area or pore-volume with the Ni loading, and this has been explained by considering the Ni to be finding the center of the DBA unit as the solitary binding site and no binding with the azine linkage. However, the anticipated shift in the PXRD spectra for such a Ni-insertion is not presented, and also the size of the Ni particles is not explicitly mentioned.<sup>14e</sup> The Ni@COF-catalyzed C–S bond cleavage on different substrates occurred with yields ranging from 26 to 99% with excellent functional group tolerance and recyclability.

### ■ COF-SUPPORTED NOBLE-METAL-BASED HETEROGENEOUS CATALYSTS

Early attempts in demonstrating the utility of COF as a porous support for catalytic metal clusters and derived organic transformations were on noble metals. In most cases, it was to demonstrate the heterogeneity of the catalyst and the efficiency, and to explore the variety of reactions it can support. Noble metals bind to heteroatoms as well as  $\pi$ -rich centers both in M(0) and M(II) oxidation states; this makes their synthesis and catalysis easy.

**Bifunctional Catalysts Using Predesigned Pyridine Groups in the COF Framework.** A bifunctional catalyst was developed by loading Pd nanoparticles into a pyridine functionalized COF (Table 3, entry 1).<sup>15a</sup> The Pd nanoparticles reside close to the pyridine functionalities, and these Pd sites cooperatively carry out a cascade catalysis wherein in step 1 the benzyl alcohol gets oxidized to benzyl aldehyde by the Pd, and in step 2, the pyridine site acts as a base to catalyze

Knoevenagel condensation between the aldehyde and the malononitrile to yield the benzylidene malononitrile product.<sup>15a</sup> The researchers had deliberately synthesized a porous polymer as well as used neat Pd salt as control catalysts, and the COF-based catalyst clearly outperformed both. Also, multiple substrates were demonstrated to work in this one-pot cascade reaction. As another bimetallic-bifunctional catalyst, Gao and co-workers, developed an imine-linked COF with 2,2'-bipyridine linkers and richly aromatic pyrene cores.<sup>15b</sup> They loaded Pd and Rh simultaneously into this COF and demonstrated that the Rh centers follow the mechanism of an already demonstrated catalyzed homogeneous reaction that involves the addition of phenylboronic acid to benzaldehyde to produce diphenylmethanol in high yield (Table 3, entry 2). The Pd<sup>2+</sup> helps oxidize this to the benzophenone. Interestingly, when they manipulated the same catalyst to have only one of the metals, the reactions occur partly and do not get completed. The presence of acetate and COD as ancillary ligands on the metal attached to the COF could be crucial to providing sufficient labile site for the catalysis. However, mild leaching (<5%) of the metals was observed after five cycles. Similar oxidative catalysis has been observed in a ruthenium-loaded imine-linked COF. Additionally, this COF also does a one-pot reaction between benzyl amine and different substitute alcohols to yield organic imines.<sup>15b</sup>

**Nitro Reduction, Suzuki Coupling Using Pd/Pt, and Au Nanoparticles @COF.** A PdCl<sub>2</sub> complex with 2,2'-bipyridine-5,5'-diamine, a linear diamine, has been directly coupled with the aldehyde, leaving the bipyridyl to line the pores. The Pd<sup>2+</sup> in the building unit gets reduced to Pd(0) during the COF formation and remains bound to the bipy

chelating site. This catalyzes the reaction between alkyne and hydroxyl-aryl halide (0.6 mol % cat., yield 70% and TON: 1100) (Table 3, entry 3).<sup>15c</sup> Dialkyl thioether appendages have been covalently linked to the walls of the imine-bonded COF, and this COF has been used as a porous medium to prepare Pt and Pd nanoparticles using NaBH<sub>4</sub> as the reducing agent and in an alcohol water medium. Interestingly, the particles have been as small as 1.7 and 1.78 nm, respectively. Excellent catalyst stability when used for nitro reductions and Suzuki–Miyaura couplings has been observed (Table 3, entry 4).<sup>16a</sup> Similar small noble metal particles have been grown inside COF by others too and have been typically investigated for hydrogen generation/nitro reduction (Table 3, entries 5–14)<sup>16b–k</sup> or Suzuki, Sonogashira coupling, or Heck couplings (Table 3, entries 15–26).<sup>16a,b,17,18</sup> In some cases, the Pd<sup>2+</sup> complex has been directly anchored to the interlayer spaces of the COF sheets, and labile groups bound to the Pd<sup>2+</sup> such as acetates or chlorides have been explained to be the substrate binding sites (Table 3, entry 18).<sup>17d</sup> When a highly hydroxyl functionalized COF was constructed, the strategic positioning and spacing of the hydroxyl yield not only binding sites to Pd, but oxidative Heck coupling takes place in a regioselective manner yielding linear products preferentially over branched ones (Table 3, entry 25).<sup>18c</sup> Similarly, multifold Heck coupling has been catalyzed by a Pd-containing amphiphilic COF containing hydrophobic ether bonds and hydrophilic triazine centers. Such a framework mimics the effect of a mixed solvent system used in homogeneous catalysis; they are typically generated by mixing a hydrophilic and a hydrophobic solvent (Table 3, entry 26).<sup>18d</sup> The resulting products are of immense industrial value.

Interestingly, in all of these above-mentioned cases, the post Pd/Pt loaded COFs have a low surface area of ~50 to 300 m<sup>2</sup>/g; yet, in many cases they have excellent catalytic activity with high yields and with good TON/TOF. In some cases, the potential of the hydrophilic–hydrophobic COF to act as a phase transfer catalyst (Table 3, entry 20)<sup>17f</sup> or an amphoteric medium is recognized (Table 3, entry 26).<sup>18d</sup> It would be easier to evaluate such possibilities if the metal-loaded COFs' pore sizes are reported from advanced porosity measurements. Encasing the Pd-loaded COF particles into a secondary support like polymer or paper or silica support or textiles and still being able to see the catalytic activity further confirm the heterogeneous character of the catalysis, and also the porosity of the COF is evident from the fact that the substrate and the reagents do reach the catalytic sites with ease even in these composite catalysts,<sup>18d</sup> and in fact such composites do not lose their rate of catalysis.<sup>16d</sup> For example, when nanofibrillated cellulose is blended with COF, it yields a highly stabilized COF, and more importantly it catalyzes the conversion of dichlorobenzene to benzene with excellent rates (0.0235 min<sup>-1</sup>) (Table 3, entry 7). It is worthy to mention that even a three-dimensional COF built from tetrahedral nodes with a relatively higher surface area (1350 m<sup>2</sup>/g) when loaded with Pd nanoparticles yields a catalytic performance comparable to the Pd@COF catalysts made using layered 2D-COFs with a much lower surface area (50–300 m<sup>2</sup>/g). This is for the Suzuki coupling reactions. Similarly, in a single study when COFs with a microporous structure (11 Å) and mesoporous structure (37 Å) were loaded with Pd nanoparticles, the resulting Pd@COF yielded a very comparable catalytic performance in terms of yield, selectivity, and conversion for the Suzuki–Miyaura coupling reaction.<sup>17b</sup>

This is against the lack of any role from the pore size or shape. This, in many cases, is because not all of the Pd nanoparticles necessarily reside in the pores, and these larger nanoparticles attached to the surface of the COF also contribute (Table 3, entry 16). Also, the pore size–shape selectivity is not truly tested. In fact, one needs to exercise some caution when it comes to Pd-based catalysts. Though they appear to be heterogeneous in nature, it is understood that the Pd can actually come out from the bulk to the surface of the catalyst and go back once the catalysis is done.<sup>17b</sup> This would make it pseudo-heterogeneous. This is true particularly for Pd but could be the case with many of them where the metal or metal-based nanoparticles size is much larger than the size of the pore. However, using the COF support could certainly provide an anchoring effect for the substrate, and it could bring the postcatalysis particles back to the host and make the recovery easier at the end. This opens up the need to investigate COF-based catalysts for more challenging organic transformations.

#### Ag@COF as Catalyst for CO<sub>2</sub> Conversion Reactions.

Another reaction that is of environmental interest is the utilization of Au or Ag @COF catalyzed organic reactions including the CO<sub>2</sub> conversion reactions.<sup>19</sup> In both cases, the propargyl alcohols were converted to cyclic organic carbonates using CO<sub>2</sub> as the reagent (Table 3, entries 27, 28). The catalysts were Ag-anchored COF. Interestingly, one was a 3D COF built from tetrahedral building units, while the other is a classical layered 2D COF. They both were microporous COFs, and the former had a surface area of 864 m<sup>2</sup>/g, which reduces to 300 m<sup>2</sup>/g with 2.3% Ag loading (Table 3, entry 27).<sup>19a</sup> The 2D COF has a surface area of 1230 m<sup>2</sup>/g, but this reduces substantially upon loading 6.3% Ag nanoparticles.<sup>19b</sup> Interestingly, the 3D COF shows a TON of ~1000, but the 2D COF shows only about 150. The 3D COF clearly seems to carry advantages: it grows smaller-sized Ag nanoparticles (2 nm for 3D vs 4–5 nm for 2D COF) and has better activity (Table 3, entries 27, 28). This can be explained considering that the smaller nanoparticles lodged in the 3D porous framework are able to expose different catalytically active facets compared to the 2D COF wherein the exposure of active facets is restricted. This is not the case with Pd/Pt nanoparticles. However, it is worth mentioning that the 2D imine-COF constructed from probably the cheapest aromatic diamine and trialdehyde, phenylenediamine, and resorcinol-trialdehyde is much more cost-effective compared to the 3D imine-COF, which is built with relatively cheaper tetrahedral aldehyde.

#### Ru or Pd@COF Subjected to Harsh Reactions.

Recently, a Ru loaded (2.4 wt %, size: 1.2 to 10 nm) imine-linked COF was employed as a catalyst for the formic acid dehydrogenation reaction.<sup>16h</sup> The Ru<sup>3+</sup> hydrates and eventually reduces to Ru(0), which becomes the active catalyst (Table 3, entry 11). The COF retains its covalent links even under this harsh acidic condition; however, the crystallinity is largely reduced, and some Ru particles sinter. A Pd-loaded COF (imine bonded), Pd@IISERP-COF1, could be used for catalyzing the CO oxidation reaction carried out up to 200 °C under N<sub>2</sub> flow or in controlled oxygen flow (Table 3, entry 26).<sup>18d</sup> The COF retained its crystallinity as well as covalent structure. This suggests that a harsh liquid medium such as acid could be more challenging for an imine-bonded COF than a high temperature (midrange) gas phase reaction.

Other classes of reactions have been carried out using noble metal-based nanoparticles embedded in a COF matrix.<sup>20a–e</sup>



For example, Pd confined in IISERP-COF1 or SDU-1 have been used to catalyze the coupling reaction between silanes and aryl iodides (Table 3, entries 26 and 29).<sup>18d,20a</sup> Telomerization of 1,3-butadiene with phenol and glycerol using Pd loaded phosphorus containing a C–C bonded microporous polymer is also reported.<sup>20f</sup> This study showed that the polymeric phosphine support outperforms the homogeneous PPh<sub>3</sub> catalyst suggesting that phosphine-based COF systems could be excellent for metal/phosphine-catalyzed reactions (Table 3, entry 34).

## CONCLUSIONS

In summary, the contemporary trend in COF-based catalysis embraces composite systems where the COF is pooled with polymeric ionic liquids, or linear-chain ionic polymers, or electronically active polymer chains. This is expected as these units bring a high density of labile groups (such as halides), which offer excellent centers for substrate binding and release, while the active functional groups like acids or bases could come from the COF walls. Under the nanoconfinement of the ordered COF pores, these two entities (host–guest) are oriented and dispersed uniformly to gain utmost cooperativity resulting in a high TON and TOF for organic transformations. This creates a dynamic pore environment that sways continuously and reversibly during the reactions. With these proven concepts, it should be possible to shoot for more complex systems that might demand high regio or chiral specificity. At the same time, exploring new as well as well-known organic transformations by replacing the classical homogeneous catalysts with COF-derived heterogeneous catalysts is a constant worthy pursuit. Meanwhile, the rapidly emerging creative modular COF designs can engage them in organic reactions which demand extreme stabilities. Also, the scalability, membranability, composite engineering, and flow-chemistry modes demonstrated in COF catalysis drive the possibility of utilizing these for truly large-scale productions in a recyclable manner. This opens up a need to investigate their particle-size, hydrophilic–hydrophobic balance-driven mass-transfer kinetics. Given all this progress, still retaining the crystallinity and thereby an ordered nanospace with undisturbed accessibility over multiple cycles (thousands to millions) remains a big challenge. The model-able structure of COF can facilitate atomic-level mechanistic simulations, but rigorous computations scrutinizing the redox/electronic dynamics of the COF are relatively uncharted. Insightful experimental–computational exploration of COF-based heterogeneous catalysis encompassing all of the developments included in this review defines the future.

## ASSOCIATED CONTENT

### Supporting Information

The Supporting Information is available free of charge at <https://pubs.acs.org/doi/10.1021/acsomega.2c00235>.

Details of the tables (PDF)

## AUTHOR INFORMATION

### Corresponding Author

Ramanathan Vaidhyanathan – Department of Chemistry and Centre for Energy Science, Indian Institute of Science Education and Research, Pune 411008, India; [orcid.org/0000-0003-4490-4397](https://orcid.org/0000-0003-4490-4397); Email: [vaidhya@acads.iiserpune.ac.in](mailto:vaidhya@acads.iiserpune.ac.in)

## Authors

Debanjan Chakraborty – Department of Chemistry and Centre for Energy Science, Indian Institute of Science Education and Research, Pune 411008, India

Dinesh Mullangi – Department of Chemistry, Indian Institute of Science Education and Research, Pune 411008, India

Chandana Chandran – Department of Chemistry, Indian Institute of Science Education and Research, Pune 411008, India

Complete contact information is available at:

<https://pubs.acs.org/10.1021/acsomega.2c00235>

## Notes

The authors declare no competing financial interest.

## Biographies

Debanjan Chakraborty obtained his doctoral degree under the guidance of Dr. Ramanathan Vaidhyanathan at the Department of Chemistry, IISER Pune, in 2020. He is currently working with Dr. Christian Serre as a postdoctoral fellow at the Institute of Porous Materials of Paris (IMAP), a joint CNRS-ENS-ESPCI laboratory. His research targets the synthesis and shaping of porous materials for CO<sub>2</sub> capture.

Dinesh Mullangi received his Master's degree in Chemistry from Pondicherry University. He carried out his Ph.D. studies in the group of Dr. R. Vaidhyanathan at IISER Pune and graduated in May 2019. Currently, he is a postdoctoral researcher working with Prof. Sir Anthony K. Cheetham at the National University of Singapore. His research interests are the development of COF and MOF-based materials for diverse nano catalytic energy conversion applications and selective separations of small molecules.

Chandana Chandran completed a BS–MS dual degree program from the Indian Institute of Science Education and Research (IISER), Pune, India, in 2021. She completed one year of M.S. thesis research under the supervision of Dr. Ramanathan Vaidhyanathan. Since 2021 September, she has been working as a project assistant in his research group. Her research interests include the synthesis of porous materials, heterogeneous catalysis, and organic transformations. Her current research is on developing COF-based single-site catalysts for organic transformations.

Dr. Ramanathan Vaidhyanathan works as an Associate Professor at IISER Pune, India. He received his Ph.D. from Jawaharlal Nehru Centre for Advanced Scientific Research (JNCASR Bangalore, India) in 2004. After his postdoctoral stays at the University of Liverpool, UK, and the University of Calgary, Canada, he joined the Department of Chemistry, IISER Pune, in 2012. His scientific interests pertain to functional porous materials (MOFs, COFs, Polymers) and their composites for gas adsorption, nanoparticle-driven catalysis, and environmental and energy applications.

## ACKNOWLEDGMENTS

We acknowledge IISER Pune for support and the funding by the “DST-Nanomission under the Thematic Unit Program” (EMR/2016/003553), the DST for material for energy storage (DST/TMD/MES/2k17/103) program, the MHRD-FAST program, and the Air Force Office of Scientific Research under Award Number FA2386-21-1-4022. D.C. thanks DST-Inspire for financial support. D.M. and C.C. acknowledge IISER Pune for funding.

## REFERENCES

- (1) (a) Feng, X.; Ding, X.; Jiang, D. Covalent organic frameworks. *Chem. Soc. Rev.* **2012**, *41*, 6010–6022. (b) Côté, A. P.; El-Kaderi, H. M.; Furukawa, H.; Hunt, J. R.; Yaghi, O. M. Reticular synthesis of microporous and mesoporous 2D covalent organic frameworks. *J. Am. Chem. Soc.* **2007**, *129*, 12914–12915. (c) Spitler, E. L.; Koo, B. T.; Novotny, J. L.; Colson, J. W.; Uribe-Romo, F. J.; Gutierrez, G. D.; Clancy, P.; Dichtel, W. R. A 2D Covalent Organic Framework with 4.7-nm Pores and Insight into Its Interlayer Stacking. *J. Am. Chem. Soc.* **2011**, *133*, 19416–19421. (d) Uribe-Romo, F. J.; Doonan, C. J.; Furukawa, H.; Oisaki, K.; Yaghi, O. M. Crystalline covalent organic frameworks with hydrazone linkages. *J. Am. Chem. Soc.* **2011**, *133*, 11478–11481. (e) Cote, A. P.; Benin, A. I.; Ockwig, N. W.; O’Keeffe, M.; Matzger, A. J.; Yaghi, O. M. Porous, crystalline, covalent organic frameworks. *Science* **2005**, *310*, 1166–1170. (f) El-Kaderi, H. M.; Hunt, J. R.; Mendoza-Cortes, J. L.; Cote, A. P.; Taylor, R. E.; O’Keeffe, M.; Yaghi, O. M. Designed synthesis of 3D covalent organic frameworks. *Science* **2007**, *316*, 268–272.
- (2) (a) Lohse, M. S.; Bein, T. Covalent Organic Frameworks: Structures, Synthesis, and Applications. *Adv. Funct. Mater.* **2018**, *28*, 1705553. (b) Huang, N.; Wang, P.; Jiang, D. Covalent organic frameworks: a materials platform for structural and functional designs. *Nat. Rev. Mater.* **2016**, *1*, 16068. (c) Diercks, S.; Yaghi, O. M. The atom, the molecule, and the covalent organic framework. *Science* **2017**, *355*, 1585. (d) Ding, S.-Y.; Wang, W. Covalent organic frameworks (COFs): from design to applications. *Chem. Soc. Rev.* **2013**, *42*, 548–568. (e) Waller, P. J.; Gándara, F.; Yaghi, O. M. Chemistry of Covalent Organic Frameworks. *Acc. Chem. Res.* **2015**, *48*, 3053–3063. (f) Kandambeth, S.; Dey, K.; Banerjee, R. Covalent Organic Frameworks: Chemistry beyond the Structure. *J. Am. Chem. Soc.* **2019**, *141*, 1807–1822.
- (3) (a) Karak, S.; Kandambeth, S.; Biswal, B. P.; Sasmal, H. S.; Kumar, S.; Pachfule, P.; Banerjee, R. Constructing Ultraporos Covalent Organic Frameworks in Seconds via an Organic Terracotta Process. *J. Am. Chem. Soc.* **2017**, *139* (5), 1856–186. (b) Mullangi, D.; Shalini, S.; Nandi, S.; Choksi, B.; Vaidhyanathan, R. Superhydrophobic covalent organic frameworks for chemical resistant coatings and hydrophobic paper and textile composites. *J. Mater. Chem. A* **2017**, *5*, 8376–8384. (c) Mullangi, D.; Dhavale, V.; Shalini, S.; Nandi, S.; Collins, S.; Woo, T.; Kurungot, S.; Vaidhyanathan, R. Low-Overpotential Electrochemical Water Splitting with Noble-Metal-Free Nanoparticles Supported in a sp<sup>3</sup> N-Rich Flexible COF. *Adv. Energy Mater.* **2016**, *6*, 1600110. (d) Nandi, S.; Singh, S. K.; Mullangi, D.; Illathvalappil, R.; George, L.; Vinod, C. P.; Kurungot, S.; Vaidhyanathan, R. Low Band Gap Benzimidazole COF Supported Ni<sub>3</sub>N as Highly Active OER Catalyst. *Adv. Energy Mater.* **2016**, *6*, 1601189. (e) Haldar, S.; Chakraborty, D.; Roy, B.; Banappanavar, G.; Rinku, K.; Mullangi, D.; Hazra, P.; Kabra, D.; Vaidhyanathan, R. Anthracene-Resorcinol Derived Covalent Organic Framework as Flexible White Light Emitter. *J. Am. Chem. Soc.* **2018**, *140*, 13367–13374. (f) Haldar, S.; Roy, K.; Kushwaha, R.; Ogale, S.; Vaidhyanathan, R. Chemical Exfoliation as a Controlled Route to Enhance the Anodic Performance of COF in LIB. *Adv. Energy Mater.* **2019**, *9*, 1902428.
- (4) (a) Wang, X.; Sun, G.; Routh, P.; Kim, D.-H.; Huang, W.; Chen, P. Heteroatom-doped graphene materials: syntheses, properties and applications. *Chem. Soc. Rev.* **2014**, *43*, 7067–7098. (b) Duan, J.; Chen, S.; Jaroniec, M.; Qiao, S. Z. Heteroatom-Doped Graphene-Based Materials for Energy-Relevant Electrocatalytic Processes. *ACS Catal.* **2015**, *5*, 5207–5234. (c) Wang, Y.; Shen, Y.; Zhou, Y.; Xue, Z.; Xi, Z.; Zhu, S. Heteroatom-Doped Graphene for Efficient NO Decomposition by Metal-Free Catalysis. *ACS Appl. Mater. Interfaces* **2018**, *10*, 36202–36210.
- (5) (a) An, K.; Somorjai, G. A. Size and Shape Control of Metal Nanoparticles for Reaction Selectivity in Catalysis. *ChemCatChem* **2012**, *4*, 1512–1524. (b) Xia, Y. N.; Xiong, Y. J.; Lim, B.; Skrabalak, S. E. Shape-controlled synthesis of metal nanocrystals: simple chemistry meets complex physics? *Angew. Chem., Int. Ed.* **2009**, *48*, 60–103. (c) Qin, G. W.; Pei, W.; Ma, X.; Xu, X.; Ren, Y.; Sun, W.; Zuo, L. Enhanced Catalytic Activity of Pt Nanomaterials: From Monodisperse Nanoparticles to Self-Organized Nanoparticle-Linked Nanowires. *J. Phys. Chem. C* **2010**, *114*, 6909–6913. (d) Somorjai, A.; Park, J. Y. Molecular Factors of Catalytic Selectivity. *Angew. Chem., Int. Ed.* **2008**, *47*, 9212–9228. (e) Pritchard, J.; Filonenko, G. A.; van Putten, R.; Hensen, E. J. M.; Pidko, E. A. Heterogeneous and homogeneous catalysis for the hydrogenation of carboxylic acid derivatives: history, advances and future directions. *Chem. Soc. Rev.* **2015**, *44*, 3808–3833. (f) Crabtree, R. H. Resolving Homogeneity Problems and Impurity Artifacts in Operationally Homogeneous Transition Metal Catalysts. *Chem. Rev.* **2012**, *112*, 1536–1554.
- (6) (a) Liu, L.; Corma, A. Metal Catalysts for Heterogeneous Catalysis: From Single Atoms to Nanoclusters and Nanoparticles. *Chem. Rev.* **2018**, *118*, 4981–5079. (b) Cui, X.; Li, W.; Ryabchuk, P.; Junge, K.; Beller, M. Bridging homogeneous and heterogeneous catalysis by heterogeneous single-metal-site catalysts. *Nat. Catal.* **2018**, *1*, 385–397. (c) White, R. J.; Luque, R.; Budarin, V. L.; Clark, J. H.; Macquarrie, D. J. Supported metal nanoparticles on porous materials. Methods and applications. *Chem. Soc. Rev.* **2009**, *38*, 481–494. (d) Rong Kim, C.; Uemura, T.; Kitagawa, S. Inorganic nanoparticles in porous coordination polymers. *Chem. Soc. Rev.* **2016**, *45*, 3828–3845. (e) Zhu, Q.-L.; Xu, Q. Immobilization of Ultrafine Metal Nanoparticles to High-Surface-Area Materials and Their Catalytic Applications. *Chem.* **2016**, *1*, 220–245. (f) Lee, H. I.; Lee, Y. Y.; Kang, D.-U.; Lee, K.; Kwon, Y.-U.; Kim, J. M. Self-arrangement of nanoparticles toward crystalline metal oxides with high surface areas and tunable 3D mesopores. *Sci. Rep.* **2016**, *6*, 21496. (g) Valtchev, V.; Tosheva, L. Porous Nanosized Particles: Preparation, Properties, and Applications. *Chem. Rev.* **2013**, *113*, 6734–6760. (h) Tessonnier, J.-P.; Ersen, O.; Weinberg, G.; Pham-Huu, C.; Su, D. S.; Schlögl, R. Selective Deposition of Metal Nanoparticles Inside or Outside Multiwalled Carbon Nanotubes. *ACS Nano* **2009**, *3*, 2081–2089. (i) Jiang, Y.; Wang, P.; Zang, X.; Yang, Y.; Kozinda, A.; Lin, L. Uniformly Embedded Metal Oxide Nanoparticles in Vertically Aligned Carbon Nanotube Forests as Pseudocapacitor Electrodes for Enhanced Energy Storage. *Nano Lett.* **2013**, *13*, 3524–3530.
- (7) (a) Wang, N.; Sun, Q.; Yu, J. Ultrasmall Metal Nanoparticles Confined within Crystalline Nanoporous Materials: A Fascinating Class of Nanocatalysts. *Adv. Mater.* **2019**, *31*, 1803966. (b) Sun, L.; Yun, Y.; Sheng, H.; Du, Y.; Ding, Y.; Wu, P.; Li, P.; Zhu, M. Rational encapsulation of atomically precise nanoclusters into metal–organic frameworks by electrostatic attraction for CO<sub>2</sub> conversion. *J. Mater. Chem. A* **2018**, *6*, 15371–15376. (c) Burkett, S. L.; Soukasene, S.; Milton, K. L.; Welch, R.; Little, A. J.; Kasi, R. M.; Coughlin, E. B. Tethered Constrained-Geometry Catalysts in Mesoporous Silica: Probing the Influence of the “Second Sphere” on Polymer Properties. *Chem. Mater.* **2005**, *17*, 2716–2723. (d) Aiyappa, H. B.; Thote, J.; Shinde, D. B.; Banerjee, R.; Kurungot, S. Cobalt-Modified Covalent Organic Framework as a Robust Water Oxidation Electrocatalyst. *Chem. Mater.* **2016**, *28*, 4375–4379.
- (8) (a) Song, Y.; Sun, Q.; Aguila, Q.; Ma, S. Opportunities of Covalent Organic Frameworks for Advanced Applications. *Adv. Sci.* **2019**, *6*, 1801410. (b) Liu, S.; Hu, C.; Liu, Y.; Zhao, X.; Pang, M.; Lin, J. One-Pot Synthesis of DOX@Covalent Organic Framework with Enhanced Chemotherapeutic Efficacy. *Chem.—Eur. J.* **2019**, *25*, 4315–4319. (c) Lin, S.; Diercks, C. S.; Zhang, Y.-B.; Kornienko, N.; Nichols, E. M.; Zhao, Y.; Paris, A. R.; Kim, D.; Yang, P.; Yaghi, O. M.; Chang, C. J. Covalent organic frameworks comprising cobalt porphyrins for catalytic CO<sub>2</sub> reduction in water. *Science* **2015**, *349*, 1208. (d) Wang, Z.; Zhang, S.; Chen, Y.; Zhang, Z.; Ma, S. Covalent organic frameworks for separation applications. *Chem. Soc. Rev.* **2020**, *49*, 708–735. (e) Das, P.; Mandal, S. K. In-Depth Experimental and Computational Investigations for Remarkable Gas/Vapor Sorption, Selectivity, and Affinity by a Porous Nitrogen-Rich Covalent Organic Framework. *Chem. Mater.* **2019**, *31*, 1584–1596. (f) Zeng, Y.; Zou, R.; Zhao, Y. Covalent Organic Frameworks for CO<sub>2</sub> Capture. *Adv. Mater.* **2016**, *28*, 2855–2873. (g) Bisbey, R. P.; Dichtel, W. R.



Covalent Organic Frameworks as a Platform for Multidimensional Polymerization. *ACS Cent. Sci.* **2017**, *3*, 533–543.

(9) (a) Knoevenagel, E. *Berichte der deutschen chemischen Gesellschaft* **1898**, *31*, 2596–2619. (b) Fang, Q.; Gu, S.; Zheng, J.; Zhuang, Z.; Qiu, S.; Yan, Y. 3D Microporous Base-Functionalized Covalent Organic Frameworks for Size-Selective Catalysis. *Angew. Chem., Int. Ed.* **2014**, *126*, 2922–2926. (c) Li, H.; Pan, Q.; Ma, Y.; Guan, X.; Xue, M.; Fang, Q.; Yan, Y.; Valtchev, V.; Qiu, S. Three-Dimensional Covalent Organic Frameworks with Dual Linkages for Bifunctional Cascade Catalysis. *J. Am. Chem. Soc.* **2016**, *138*, 14783–14788. (d) Shinde, D. B.; Kandambeth, S.; Pachfule, P.; Kumar, R. R. I.; Banerjee, R. Bifunctional covalent organic frameworks with two dimensional organocatalytic micropores. *Chem. Commun.* **2015**, *51*, 310–313. (e) Ma, Y.-X.; Li, Z.-J.; Wei, L.; Ding, S.-Y.; Zhang, Y.-B.; Wang, W. A Dynamic Three-Dimensional Covalent Organic Framework. *J. Am. Chem. Soc.* **2017**, *139*, 4995–4998. (f) Luis-Barrera, J.; Cano, R.; Imani-Shakibaei, G.; Heras-Domingo, J.; Pérez-Carvajal, J.; Imaz, I.; Maspoch, D.; Solans-Monfort, X.; Alemán, J.; Mas-Ballesté, R. Switching acidic and basic catalysis through supramolecular functionalization in a porous 3D covalent imine-based material. *Catal. Sci. Technol.* **2019**, *9*, 6007–6014.

(10) (a) Bara, J. E.; Camper, D. E.; Gin, D. L.; Noble, R. D. Room-Temperature Ionic Liquids and Composite Materials: Platform Technologies for CO<sub>2</sub> Capture. *Acc. Chem. Res.* **2010**, *43*, 152–159. (b) Bates, E. D.; Mayton, R. D.; Ntai, I. H.; Davis, J. H. CO<sub>2</sub> Capture by a Task-Specific Ionic Liquid. *J. Am. Chem. Soc.* **2002**, *124*, 926–927. (c) Ding, L.-G.; Yao, B.-J.; Li, F.; Shi, S.-C.; Huang, N.; Yin, H.-B.; Guan, Q.; Dong, Y.-B. Ionic liquid-decorated COF and its covalent composite aerogel for selective CO<sub>2</sub> adsorption and catalytic conversion. *J. Mater. Chem. A* **2019**, *7*, 4689–4698. (d) Saptal, V.; Shinde, D. B.; Banerjee, R.; Bhanage, B. M. State-of-the-art catechol porphyrin COF catalyst for chemical fixation of carbon dioxide via cyclic carbonates and oxazolidinones. *Catal. Sci. Technol.* **2016**, *6*, 6152–6158. (e) Mu, Z.-J.; Ding, X.; Chen, Z.-Y.; Han, B.-H. Zwitterionic Covalent Organic Frameworks as Catalysts for Hierarchical Reduction of CO<sub>2</sub> with Amine and Hydrosilane. *ACS Appl. Mater. Interfaces* **2018**, *10*, 41350–41358. (f) Zhi, Y.; Shao, P.; Feng, X.; Xia, H.; Zhang, Y.; Shi, Z.; Mu, Y.; Liu, X. Covalent organic frameworks: efficient, metal-free, heterogeneous organocatalysts for chemical fixation of CO<sub>2</sub> under mild conditions. *J. Mater. Chem. A* **2018**, *6*, 374–382.

(11) (a) Sun, Q.; Tang, Y.; Aguila, B.; Wang, S.; Xiao, F.-S.; Thallapally, P. K.; Al-Enizi, A. M.; Nafady, A.; Ma, S. Reaction Environment Modification in Covalent Organic Frameworks for Catalytic Performance Enhancement. *Angew. Chem., Int. Ed.* **2019**, *131*, 8762–8767. (b) Mullangi, D.; Chakraborty, D.; Pradeep, A.; Koshti, V.; Vinod, C. P.; Panja, S.; Nair, S.; Vaidhyanathan, R. Highly Stable COF-Supported Co/Co(OH)<sub>2</sub> Nanoparticles Heterogeneous Catalyst for Reduction of Nitrile/Nitro Compounds under Mild Conditions. *Small* **2018**, *14*, 1801233. (c) Peng, Y.; Hu, Z.; Gao, Y.; Yuan, D.; Kang, Z.; Qian, Y.; Yan, N.; Zhao, D. Synthesis of a Sulfonated Two-Dimensional Covalent Organic Framework as an Efficient Solid Acid Catalyst for Biobased Chemical Conversion. *ChemSusChem* **2015**, *8*, 3208–3212. (d) Little, R. D.; Masjedizadeh, M. R.; Wallquist, O.; McLoughlin, J. I. The Intramolecular Michael Reaction. *Org. React.* **1995**, *47*, 315–552. (e) Mather, B. D.; Viswanathan, K.; Miller, K.; Long, T. E. Michael addition reactions in macromolecular design for emerging technologies. *Prog. Polym. Sci.* **2006**, *31*, 487–531. (f) Xu, H.; Chen, X.; Gao, J.; Lin, J.; Addicoat, M.; Irlé, S.; Jiang, D. Catalytic covalent organic frameworks via pore surface engineering. *Chem. Commun.* **2014**, *50*, 1292–1294. (g) Li, X.; Wang, Z.; Sun, J.; Gao, J.; Zhao, Y.; Cheng, P.; Aguila, B.; Ma, S.; Chen, Y.; Zhang, Z. Squaramide-decorated covalent organic framework as a new platform for biomimetic hydrogen-bonding organocatalysis. *Chem. Commun.* **2019**, *55*, 5423–5426. (h) Wu, Y.; Xu, H.; Chen, X.; Gao, J.; Jiang, D. A  $\pi$ -electronic covalent organic framework catalyst:  $\pi$ -walls as catalytic beds for Diels–Alder reactions under ambient conditions. *Chem. Commun.* **2015**, *51*, 10096–10098. (i) Shen, J.-C.; Jiang, W.-L.; Guo, W.-D.; Qi, Q.-Y.; Ma, D.-L.; Lou,

X.; Shen, M.; Hu, B.; Yang, H.-B.; Zhao, X. A rings-in-pores net-crown ether-based covalent organic frameworks for phase-transfer catalysis. *Chem. Commun.* **2020**, *56*, 595–598.

(12) (a) Sharma, R. K.; Yadav, P.; Yadav, M.; Gupta, R.; Rana, P.; Srivastava, A.; Zbořil, R.; Varma, R. S.; Antonietti, M.; Gawande, M. B. Recent development of covalent organic frameworks (COFs): synthesis and catalytic (organic-electro-photo) applications. *Mater. Horiz.* **2020**, *7*, 411–454. (b) Gao, W.; Sun, X.; Niu, H.; Song, X.; Li, K.; Gao, H.; Zhang, W.; Yu, J.; Jia, M. Phosphomolybdc acid functionalized covalent organic frameworks: Structure characterization and catalytic properties in olefin epoxidation. *Microporous Mesoporous Mater.* **2015**, *213*, 59–67. (c) Zhang, W.; Jiang, P.; Wang, Y.; Zhang, J.; Gao, Y.; Zhang, P. Bottom-up approach to engineer a molybdenum-doped covalent-organic framework catalyst for selective oxidation reaction. *RSC Adv.* **2014**, *4*, 51544–51547. (d) Mu, M.; Wang, Y.; Qin, Y.; Yan, X.; Li, Y.; Chen, L. Two-Dimensional Imine-Linked Covalent Organic Frameworks as a Platform for Selective Oxidation of Olefins. *ACS Appl. Mater. Interfaces* **2017**, *9*, 22856–22863. (e) Zhao, M.; Wu, C.-D. Synthesis and post-metallation of a covalent-porphyrinic framework for highly efficient aerobic epoxidation of olefins. *Catal. Commun.* **2017**, *99*, 146–149. (f) Yu, D.; Gao, W.; Xing, S.; Lian, L.; Zhang, H.; Wang, X.; Lou, D. Fe-doped H<sub>3</sub>PMo<sub>12</sub>O<sub>40</sub> immobilized on covalent organic frameworks (Fe/PMA@COFs): a heterogeneous catalyst for the epoxidation of cyclooctene with H<sub>2</sub>O<sub>2</sub>. *RSC Adv.* **2019**, *9*, 4884–4891. (g) Zhang, W.; Jiang, P.; Wang, Y.; Zhang, J.; Zhang, P. Bottom-up approach to engineer two covalent porphyrinic frameworks as effective catalysts for selective oxidation. *Catal. Sci. Technol.* **2015**, *5*, 101–104. (h) Wang, X.-S.; Chrzanowski, M.; Yuan, D.; Sweeting, B. S.; Ma, S. Covalent Heme Framework as a Highly Active Heterogeneous Biomimetic Oxidation Catalyst. *Chem. Mater.* **2014**, *26*, 1639–1644.

(13) (a) Chakraborty, D.; Nandi, S.; Mullangi, D.; Haldar, S.; Vinod, C. P.; Vaidhyanathan, R. Cu/Cu<sub>2</sub>O Nanoparticles Supported on a Phenol–Pyridyl COF as a Heterogeneous Catalyst for the Synthesis of Unsymmetrical Dienes via Glaser–Hay Coupling. *ACS Appl. Mater. Interfaces* **2019**, *11*, 15670–15679. (b) Qiao, J. X.; Lam, P. Y. S. Recent Advances in Chan–Lam Coupling Reaction: Copper-Promoted C–Heteroatom Bond Cross-Coupling Reactions with Boronic Acids and Derivatives. In *Boronic Acids: Preparation and Applications in Organic Synthesis, Medicine and Materials*, 1&2, 2nd edition; Hall, D. G., Ed.; Wiley-VCH, 2011. DOI: DOI: 10.1002/9783527639328. (c) Han, Y.; Zhang, M.; Zhang, Y.-Q.; Zhang, Z.-H. Copper immobilized at a covalent organic framework: an efficient and recyclable heterogeneous catalyst for the Chan–Lam coupling reaction of aryl boronic acids and amines. *Green Chem.* **2018**, *20*, 4891–4900. (d) Pastor, I. M.; Yus, M. The Prins Reaction: Advances and Applications. *Curr. Org. Chem.* **2007**, *11*, 925. (e) Vardhan, H.; Verma, G.; Ramani, S.; Nafady, A.; Al-Enizi, A. M.; Pan, Y.; Yang, Z.; Yang, H.; Ma, S. Covalent Organic Framework Decorated with Vanadium as a New Platform for Prins Reaction and Sulfide Oxidation. *ACS Appl. Mater. Interfaces* **2019**, *11*, 3070–3079. (f) Vardhan, H.; Hou, L.; Yee, E.; Nafady, A.; Al-Abdrabnabi, M. A.; Al-Enizi, A. M.; Pan, Y.; Yang, Z.; Ma, S. Vanadium Docked Covalent-Organic Frameworks: An Effective Heterogeneous Catalyst for Modified Mannich-Type Reaction. *ACS Sustainable Chem. Eng.* **2019**, *7*, 4878–4888.

(14) (a) Rodriguez, N.; Goossen, L. Decarboxylative coupling reactions: a modern strategy for C–C-bond formation. *Chem. Soc. Rev.* **2011**, *40*, 5030–5048. (b) Cifuentes, J. M. C.; Ferreira, B. X.; Esteves, P. M.; Buarque, C. D. Decarboxylative Cross-Coupling of Cinnamic Acids Catalyzed by Iron-Based Covalent Organic Frameworks. *Top. Catal.* **2018**, *61*, 689–698. (c) Maia, R. A.; Berg, F.; Ritleng, V.; Louis, B.; Esteves, P. M. Design, Synthesis and Characterization of Nickel-Functionalized Covalent Organic Framework NiCl@RIO-12 for Heterogeneous Suzuki–Miyaura Catalysis. *Chem.—Eur. J.* **2020**, *26*, 2051–2059. (d) Chandran, D.; Bae, C.; Ahn, I.; Ha, C.-S.; Kim, I. Neutral Ni(II) complexes based on keto-enamine salicylideneanilines active for selective dimerization of ethylene. *J. Organomet. Chem.* **2009**, *694*, 1254–1258. (e) Haug, W.

K.; Wolfson, E. R.; Morman, B. T.; Thomas, C. M.; McGrier, P. L. A Nickel-Doped Dehydrobenzoannulene-Based Two-Dimensional Covalent Organic Framework for the Reductive Cleavage of Inert Aryl C–S Bonds. *J. Am. Chem. Soc.* **2020**, *142*, 5521–5525. (f) Ma, Y.; Liu, X.; Guan, X.; Li, H.; Yusran, Y.; Xue, M.; Fang, Q.; Yan, Y.; Qiu, S.; Valtchev, V. One-pot cascade syntheses of microporous and mesoporous pyrazine-linked covalent organic frameworks as Lewis-acid catalysts. *Dalton Trans.* **2019**, *48*, 7352–7357.

(15) (a) Sun, Q.; Aguila, B.; Ma, S. A bifunctional covalent organic framework as an efficient platform for cascade catalysis. *Mater. Chem. Front.* **2017**, *1*, 1310–1316. (b) Leng, W.; Peng, Y.; Zhang, J.; Lu, H.; Feng, X.; Ge, R.; Dong, B.; Wang, B.; Hu, X.; Gao, Y. Sophisticated Design of Covalent Organic Frameworks with Controllable Bimetallic Docking for a Cascade Reaction. *Chem.—Eur. J.* **2016**, *22*, 9087–9091. (c) Bhadra, M.; Sasmal, H. S.; Basu, A.; Midya, S. P.; Kandambeth, S.; Pachfule, P.; Balaraman, E.; Banerjee, R. Pre-designed Metal-Anchored Building Block for In Situ Generation of Pd Nanoparticles in Porous Covalent Organic Framework: Application in Heterogeneous Tandem Catalysis. *ACS Appl. Mater. Interfaces* **2017**, *9*, 13785–13792.

(16) (a) Lu, S.; Hu, Y.; Wan, S.; McCaffrey, R.; Jin, Y.; Gu, H.; Zhang, W. Synthesis of Ultrafine and Highly Dispersed Metal Nanoparticles Confined in a Thioether-Containing Covalent Organic Framework and Their Catalytic Applications. *J. Am. Chem. Soc.* **2017**, *139* (47), 17082–17088. (b) Shi, X.; Yao, Y.; Xu, Y.; Liu, K.; Zhu, G.; Chi, L.; Lu, G. Imparting Catalytic Activity to a Covalent Organic Framework Material by Nanoparticle Encapsulation. *ACS Appl. Mater. Interfaces* **2017**, *9*, 7481–7488. (c) Pachfule, P.; Kandambeth, S.; Diaz, D. D.; Banerjee, R. Highly stable covalent organic framework–Au nanoparticles hybrids for enhanced activity for nitrophenol reduction. *Chem. Commun.* **2014**, *50*, 3169–3172. (d) Wan, X.; Wang, X.; Chen, G.; Guo, C.; Zhang, B. Covalent organic framework/nanofibrillated cellulose composite membrane loaded with Pd nanoparticles for dechlorination of dichlorobenzene. *Mater. Chem. Phys.* **2020**, *246*, 122574. (e) Tan, X.; Zeng, W.; Fan, Y.; Yan, J.; Zhao, G. Covalent organic frameworks bearing pillar[6]arene-reduced Au nanoparticles for the catalytic reduction of nitroaromatics. *Nanotechnology* **2020**, *31*, 135705. (f) Li, X.; Zhang, C.; Luo, M.; Yao, Q.; Lu, Z.-H. Ultrafine Rh nanoparticles confined by nitrogen-rich covalent organic frameworks for methanolysis of ammonia borane. *Inorg. Chem. Front.* **2020**, *7*, 1298–1306. (g) Tao, R.; Shen, X.; Hu, Y.; Kang, K.; Zheng, Y.; Luo, S.; Yang, S.; Li, W.; Lu, S.; Jin, Y.; Qiu, L.; Zhang, W. Phosphine-Based Covalent Organic Framework for the Controlled Synthesis of Broad-Scope Ultrafine Nanoparticles. *Small* **2020**, *16*, 1906005. (h) Gonçalves, L. P. L.; Christensen, D. B.; Meledina, M.; Salonen, L. M.; Petrovykh, D. Y.; Carbó-Argibay, E.; Sousa, J. P. S.; Soares, O. S. G. P.; Pereira, M. F. R.; Kegnæs, S.; Kolen'ko, Y. V. Selective formic acid dehydrogenation at low temperature over a RuO<sub>2</sub>/COF pre-catalyst synthesized on the gram scale. *Catal. Sci. Technol.* **2020**, *10*, 1991–1995. (i) Zhang, Q.-P.; Sun, Y.-L.; Cheng, G.; Wang, Z.; Ma, H.; Ding, S.-Y.; Tan, B.; Bu, J.-h.; Zhang, C. Highly dispersed gold nanoparticles anchoring on post-modified covalent organic framework for catalytic application. *Chem. Eng. J.* **2020**, *391*, 123471. (j) Gong, W.; Wu, Q.; Jiang, G.; Li, G. Ultrafine silver nanoparticles supported on a covalent carbazole framework as high-efficiency nanocatalysts for nitrophenol reduction. *J. Mater. Chem. A* **2019**, *7*, 13449–13454. (k) Ding, Z.-D.; Wang, Y.-X.; Xi, S.-F.; Li, Y.; Li, Z.; Ren, X.; Gu, Z.-G. A Hexagonal Covalent Porphyrin Framework as an Efficient Support for Gold Nanoparticles toward Catalytic Reduction of 4-Nitrophenol. *Chem.—Eur. J.* **2016**, *22*, 17029–17036.

(17) (a) Gonçalves, R. S. B.; de Oliveira, A. B. V.; Sindra, H. C.; Archanjo, B. S.; Mendoza, M. E.; Carneiro, L. S. A.; Buarque, C. D.; Esteves, P. M. Heterogeneous Catalysis by Covalent Organic Frameworks (COF): Pd(OAc)<sub>2</sub>@COF-300 in Cross-Coupling Reaction. *ChemCatChem* **2016**, *8*, 743–750. (b) Kaleeswaran, D.; Antony, R.; Sharma, A.; Malani, A.; Murugavel, R. Catalysis and CO<sub>2</sub> Capture by Palladium-Incorporated Covalent Organic Frameworks. *ChemPlusChem* **2017**, *82*, 1253–1265. (c) Zhu, W.; Wang, X.; Li, T.;

Shen, R.; Hao, S.-J.; Li, Y.; Wang, Q.; Li, Z.; Gu, Z.-G. Porphyrin-based porous polyimide polymer/Pd nanoparticle composites as efficient catalysts for Suzuki–Miyaura coupling reactions. *Polym. Chem.* **2018**, *9*, 1430–1438. (d) Ding, S.-Y.; Gao, J.; Wang, Q.; Zhang, Y.; Song, W.-G.; Su, C.-Y.; Wang, W. Construction of Covalent Organic Framework for Catalysis: Pd/COF-LZU1 in Suzuki–Miyaura Coupling Reaction. *J. Am. Chem. Soc.* **2011**, *133*, 19816–19822. (e) Hou, Y.; Zhang, X.; Sun, J.; Lin, S.; Qi, D.; Hong, R.; Li, D.; Xiao, X.; Jiang, J. Good Suzuki-coupling reaction performance of Pd immobilized at the metal-free porphyrin-based covalent organic framework. *Microporous Mesoporous Mater.* **2015**, *214*, 108–114. (f) Wang, J.-C.; Liu, C.-X.; Kan, X.; Wu, X.-W.; Kan, J.-L.; Dong, Y.-B. Pd@COF-QA: a phase transfer composite catalyst for aqueous Suzuki–Miyaura coupling reaction. *Green Chem.* **2020**, *22*, 1150–1155. (g) Yang, J.; Wu, Y.; Wu, X.; Liu, W.; Wang, Y.; Wang, J. An N-heterocyclic carbene-functionalised covalent organic framework with atomically dispersed palladium for coupling reactions under mild conditions. *Green Chem.* **2019**, *21*, 5267–5273. (h) Sadhasivam, V.; Balasaravanan, R.; Chithiraikumar, C.; Siva, A. Incorporating Pd(OAc)<sub>2</sub> on Imine Functionalized Microporous Covalent Organic Frameworks: A Stable and Efficient Heterogeneous Catalyst for Suzuki–Miyaura Coupling in Aqueous Medium. *Chem. Select* **2017**, *2*, 1063–1070.

(18) (a) Pachfule, P.; Panda, M. K.; Kandambeth, S.; Shivaprasad, S. M.; Diaz, D. D.; Banerjee, R. Multifunctional and robust covalent organic framework–nanoparticle hybrids. *J. Mater. Chem. A* **2014**, *2*, 7944–7952. (b) Leng, W.; Ge, R.; Dong, B.; Wang, C.; Gao, Y. Bimetallic docked covalent organic frameworks with high catalytic performance towards tandem reactions. *RSC Adv.* **2016**, *6*, 37403–37406. (c) Han, J.; Sun, X.; Wang, X.; Wang, Q.; Hou, S.; Song, X.; Wei, Y.; Wang, R.; Ji, W. Covalent Organic Framework as a Heterogeneous Ligand for the Regioselective Oxidative Heck Reaction. *Org. Lett.* **2020**, *22*, 1480–1484. (d) Mullangi, D.; Nandi, S.; Shalini, S.; Sreedhala, S.; Vinod, C. P.; Vaidhyanathan, R. Pd loaded amphiphilic COF as catalyst for multi-fold Heck reactions, C–C couplings and CO oxidation. *Sci. Rep.* **2015**, *5*, 10876.

(19) (a) Guan, P.; Qiu, J.; Zhao, Y.; Wang, H.; Li, Z.; Shi, Y.; Wang, J. A novel crystalline azine-linked three-dimensional covalent organic framework for CO<sub>2</sub> capture and conversion. *Chem. Commun.* **2019**, *55*, 12459–12462. (b) Chakraborty, D.; Shekhar, P.; Singh, H. D.; Kushwaha, R.; Vinod, C. P.; Vaidhyanathan, R. Ag Nanoparticles Supported on a Resorcinol-Phenylenediamine-Based Covalent Organic Framework for Chemical Fixation of CO<sub>2</sub>. *Chem.—Asian J.* **2019**, *14*, 4767–4773.

(20) (a) Lin, S.; Hou, Y.; Deng, X.; Wang, H.; Sun, S.; Zhang, X. A triazine-based covalent organic framework/palladium hybrid for one-pot silicon-based cross-coupling of silanes and aryl iodides. *RSC Adv.* **2015**, *5*, 41017–41024. (b) Chen, G.-J.; Li, X.-B.; Zhao, C.-C.; Ma, H.-C.; Kan, J.-L.; Xin, Y.-B.; Chen, C.-X.; Dong, Y.-B. Ru Nanoparticles-Loaded Covalent Organic Framework for Solvent-Free One-Pot Tandem Reactions in Air. *Inorg. Chem.* **2018**, *57*, 2678–2685. (c) Pan, S.; Yao, D.; Liang, A.; Wen, G.; Jiang, Z. New Ag-Doped COF Catalytic Amplification Aptamer Analytical Platform for Trace Small Molecules with the Resonance Rayleigh Scattering Technique. *ACS Appl. Mater. Interfaces* **2020**, *12*, 12120–12132. (d) Heintz, P. M.; Schumacher, B. P.; Chen, M.; Huang, W.; Stanley, L. M. A Pd(II)-Functionalized Covalent Organic Framework for Catalytic Conjugate Additions of Arylboronic Acids to  $\beta,\beta$ -Disubstituted Enones. *ChemCatChem.* **2019**, *11*, 4286–4290. (e) Vardhan, H.; Pan, Y.; Yang, Z.; Verma, G.; Nafady, A.; Al-Enizi, A. M.; Alotaibi, T. M.; Almaghrabi, O. A.; Ma, S. Iridium complex immobilization on covalent organic framework for effective C–H borylation. *APL Mater.* **2019**, *7*, 101111. (f) Hausoul, P. J. C.; Eggenhuisen, T. M.; Nand, D.; Baldus, M.; Weckhuysen, B. M.; Gebbink, R. J. M. K.; Bruijninx, P. C. A. Development of a 4,4'-biphenyl/phosphine-based COF for the heterogeneous Pd-catalysed telomerisation of 1,3-butadiene. *Catal. Sci. Technol.* **2013**, *3*, 2571–2579.